THE UNIVERSITY OF MICHIGAN

6633-1-T

Derivation of Aerospace Antenna Coupling-Factor Interference Prediction Techniques

Interim Report No. 1

1 June through 30 November 1964

Approved J. A. M. Lyon

J. A. M. Lyon
Professor, Electrical Engineering

December 1964

Contract No. AF-33(615)-1761

Proj. 4357, Task 435705

Air Force Avionics Laboratory, AVWC
Research and Technology Division, AFSC
Wright-Patterson Air Force Base, Ohio 45433

FOREWORD

This report was prepared by The University of Michigan under USAF Contract No. AF-33(615)-1761, Task 435705, Project 4357. The work was administered under the direction of the Air Force Avionics Laboratory, Research and Technology Division, Air Force Systems Command, E. M. Turner, Technical Manager; Olin E. Horton, Project Engineer.

This Report covers work conducted from June through November 1964.

TABLE OF CONTENTS

	ABSTRACT	iv
I	INTRODUCTION	1
II	THEORETICAL DERIVATION OF COUPLING	4
	2.1 E-Sectoral Horns	4
	2.2 H-Sectoral Horns	12
	2.3 Conical Horns	18
	2.4 General Analysis of Sectoral Horn Coupling	26
III	EXPERIMENTAL COUPLING DATA	44
	3.1 E- and H-Sectoral Horns	44
	3.2 Conical and Pyramidal Horns	47
IV	CONCLUSIONS	52
V	FUTURE WORK	53
	REFERENCES	55

ABSTRACT

The progress which has been made in the determination of power interference between two similar antennas is described and both theoretical and experimental results are given. Mathematical methods are presented showing the coupling between one rectangular aperture and another. The methods are also extended to the case of the coupling between two conical horns. Good confirmation has been achieved between experimental and theoretical results.

In some situations, the coupling will be below the -75 db value which has been given by the sponsor to indicate the range of interest for the measurements. Studies have been undertaken to determine the influence of scattering by auxiliary bodies or protuberances.

Methods of data presentation involving nomographs and computer programs are discussed under future work.

I

INTRODUCTION

The present investigation of the coupling between horn antennas is a continuation of work performed on an earlier contract for the same sponsor. The previous work, summarized by Khan et al (1964), was largely concerned with coupling problems involving slot and spiral antennas. Some attention was also given to dielectric rod and horn antennas. This report presents a more detailed investigation of horn coupling behavior.

Theoretical and experimental work has been performed to predict the coupling between identical horns of the E- and H-sectoral, pyramidal and conical types. Pairs of these horns were constructed and experimental patterns were measured.

Due to the large number of possible designs of these types of horns, one cannot expect to cover the complete coupling problem with an experimental program. Consequently, much emphasis was placed on the construction of theoretical models which could be used to provide coupling data. The experimental coupling patterns were then used to spot-check the theoretical data. Preliminary checks of the theoretical coupling patterns indicate a high correlation with experimental data. It is hoped that the mathematical models can be used to provide coupling data for a wide range of operating frequencies for each of the four horn types mentioned with any specific set of design parameters. In the following sections the theoretical models are derived and the resulting coupling patterns are compared with experimentally measured patterns. In addition, many experimental coupling patterns are presented and analyzed.

Throughout the following sections, reference is made to E- and H-plane coupling. E-plane coupling refers to the situation in which the E-field directions in the two horns are colinear at the beginning of the measurement ($\phi = 0$). One antenna is then rotated as the coupling pattern is taken. Similarly, the term

H-plane coupling signifies an orientation in which the H-fields in the two horns are colinear when $\phi = 90^{o}$ (Fig. 1).

In Sections 2.1 and 2.2 expressions for the far field coupling between E- and H-sectoral horns are derived and theoretical and experimental results are compared. In Section 2.3 a theoretical expression for the far field coupling between conical horns is derived. In Section 2.4, the coupling between two sectoral horns is considered using a more unified approach to provide expressions which are valid in both the near and far regions. In Section III experimental coupling results are presented for E- and H-sectoral horns, for conical horns and for pyramidal horns - each for three X-band frequencies. In Section IV we present the conclusions of our study up to the report period and Section V discusses the work planned for the remainder of this contract.

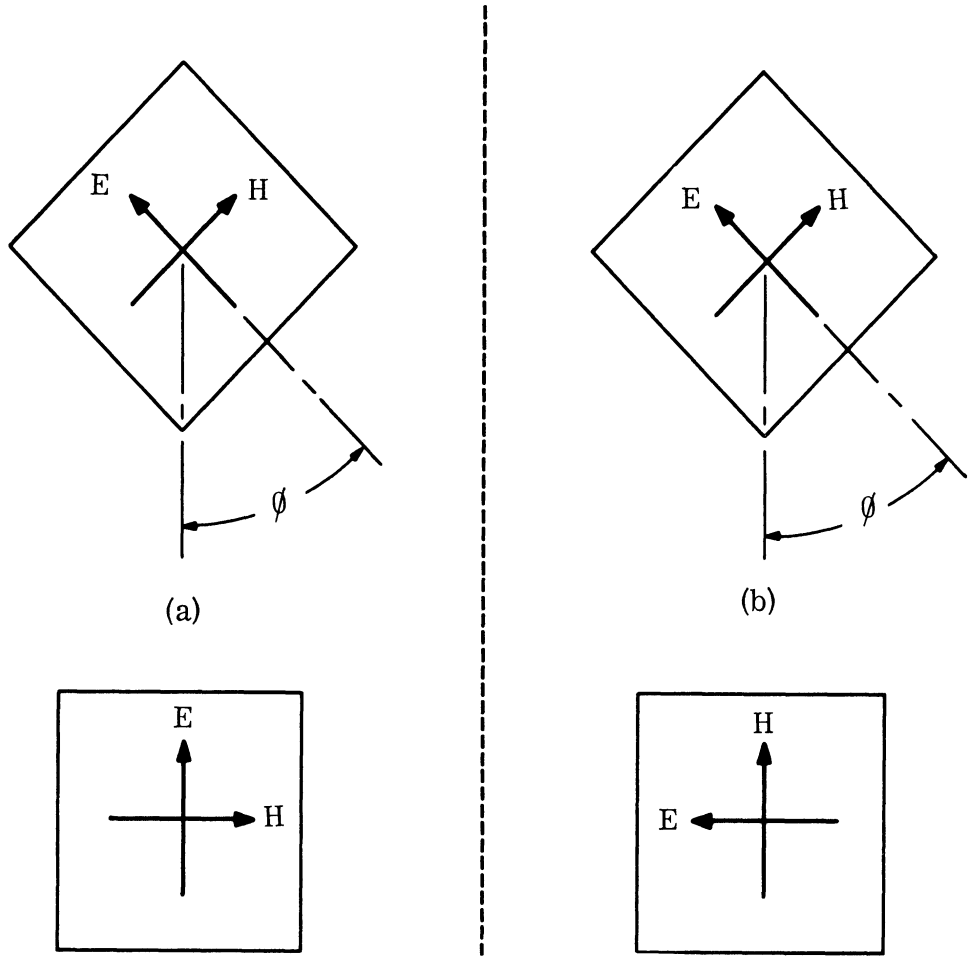

FIG. 1: DIFFERENTIATION BETWEEN E- AND H-PLANE COUPLING.

II

THEORETICAL DERIVATION OF COUPLING

2.1 E-sectoral Horns

In this section, an expression is derived for the far field coupling between E-sectoral horns. The horns are flush mounted in an infinitely conducting ground plane of infinite extent and operate in the fundamental TE_{10} mode.

One proceeds by first calculating the radiation fields on the ground plane produced by the transmitting antenna with the receiving antenna absent. The coordinate system is shown in Figure 2. According to the fundamental existence theorem of electromagnetic theory, a uniquely determined electromagnetic field exists provided the tangential component of either the electric, or the magnetic field is specified at each point (including discontinuity points) of a surface bounding a given region. For the present problem, the tangential electric field $\bar{E} \times \hat{n}$ vanishes on the ground plane and along the infinite hemisphere centered about the origin, and it has the value $\bar{M}$ in the aperture. The field in the aperture is equivalent to a magnetic surface current distribution on a conductor of density $\bar{M}$. By employing the duality of electric current and magnetic current, we obtain the Hertzian magnetic vector in the form (Stratton, 1941),

$$\bar{\pi}^* = \frac{1}{2\pi j\omega\mu} \iint_{\text{aperture}} \bar{M}(\bar{r}') \frac{e^{-jk|\bar{R}-\bar{r}'|}}{|\bar{R}-\bar{r}'|} dS', \tag{1}$$

where a factor of 2 resulting from imaging effect is also taken into account (Lewin, 1951). Using this magnetic Hertzian potential, the electric and magnetic fields in the half space are given by (Stratton, 1941)

$$\bar{E} = -j\omega\mu \nabla \times \bar{\pi}^* \tag{2}$$

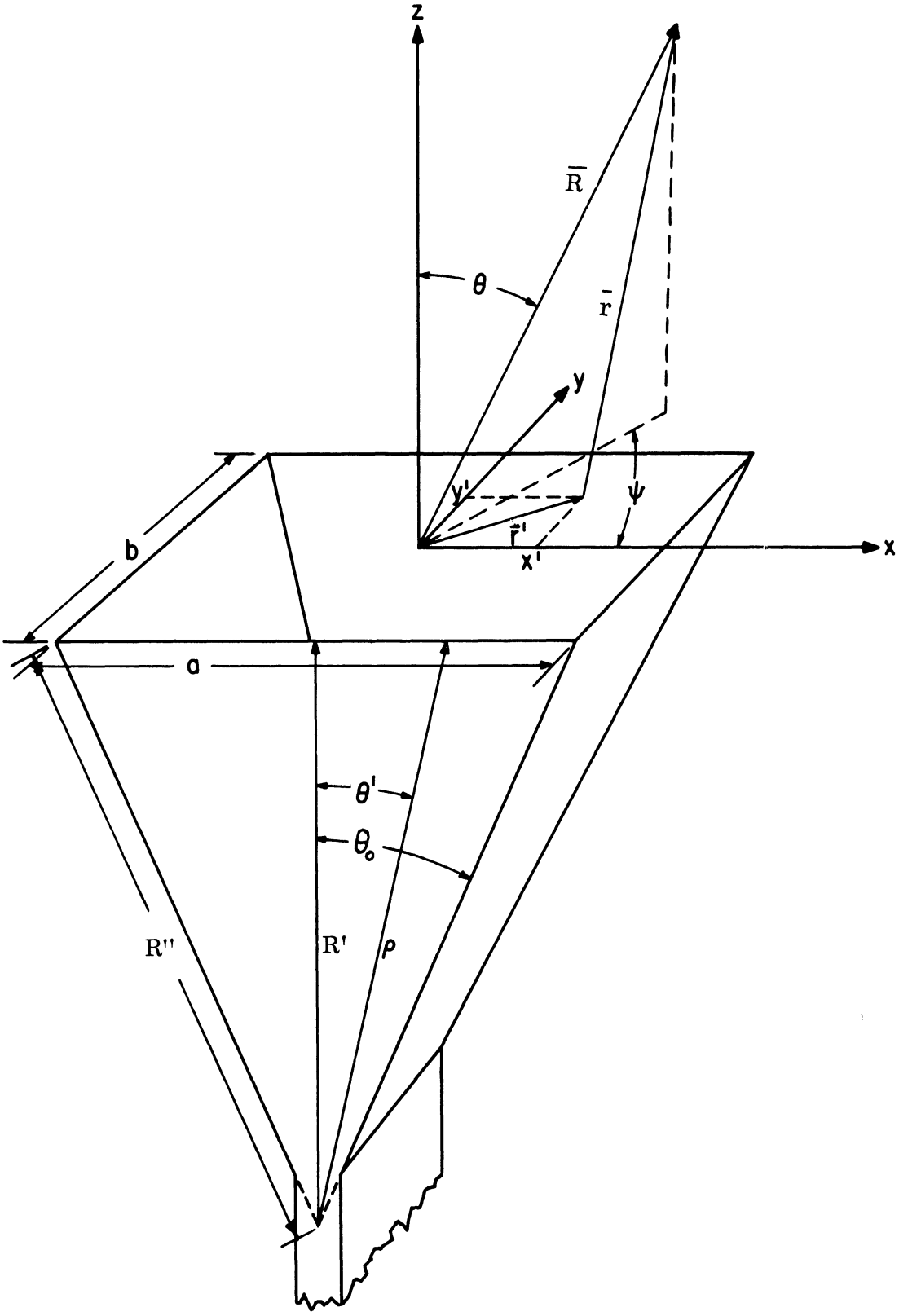

FIG. 2: E-SECTORAL HORN GEOMETRY

$$\bar{H} = \nabla (\nabla \cdot \bar{\pi}^*) + k^2 \bar{\pi}^* \tag{3}$$

where

$$k^2 = \omega^2 \mu \epsilon \quad .$$

At this point it was necessary to assume a distribution for the electric field in the aperture of the horn. The distribution chosen was

$$\bar{E}_x = E_o \cos \frac{\pi y'}{b} e^{-jk_g \sqrt{x'^2 + R'^2}} \hat{x} \quad , \tag{4}$$

where k_g is the waveguide propagation factor and the other variables are shown in Figure 2. This distribution is the result of the assumption that the wave fronts in the horn are circular and that the basic cosine variation of the field with y' in the waveguide is transmitted to the horn.

The magnetic current $\bar{M}$ is then given by

$$\bar{M} = \bar{E} \times \hat{n} = \bar{E}_x \times \hat{z} = -\bar{E}_x \hat{y} \quad .$$

From (1) the magnetic Hertzian vector becomes

$$\bar{\pi}^* = \pi_y^* \hat{y} = \frac{-\hat{y} E_o}{2\pi j \omega \mu} \int_{-b/2}^{b/2} \int_{-a/2}^{a/2} \cos \frac{\pi y'}{b} \frac{e^{-j(kr + k_g \sqrt{x'^2 + R'^2})}}{r} dx' dy' \tag{5}$$

where

$$r = |\bar{r}| = |\bar{R} - \bar{r}'|$$

In order to derive the electric fields, the curl of the Hertzian vector must be evaluated:

$$\nabla \times \bar{\pi}^* = \nabla \times \pi_y^* \hat{y} = -\frac{\partial \pi_y^*}{\partial z} \hat{x} + \frac{\partial \pi_y^*}{\partial x} \hat{z} \quad . \tag{6}$$

For coupling purposes, we are interested only in the fields on the ground plane. The x component of $\nabla \times \bar{\pi}^*$ is, therefore, neglected leaving

$$(\nabla \times \bar{\pi}^*)_z = \frac{\partial \pi_y^*}{\partial x} \quad . \tag{7}$$

Applying (7) to (5), the partial derivative with respect to x may be taken inside the integrals to give

$$(\nabla \times \bar{\pi}^*)_z = \frac{-E_o}{2\pi j\omega\mu} \int_{-a/2}^{a/2} \int_{-b/2}^{b/2} \cos \frac{\pi y'}{b} \exp\left[-jk_g\sqrt{x'^2+R'^2}\right] \cdot \frac{\partial}{\partial x}\left(\frac{e^{-jkr}}{r}\right) dx'\,dy' \quad . \tag{8}$$

If the differentiation is carried out, one obtains

$$\frac{\partial}{\partial x}\left(\frac{e^{-jkr}}{r}\right) = -\frac{(x-x')e^{-jkr}}{r^2}\left(jk + \frac{1}{r}\right) \quad .$$

Therefore, equation (8) becomes

$$(\nabla \times \bar{\pi}^*)_z = \frac{E_o}{2\pi j\omega\mu}\left[jk \int_{-a/2}^{a/2} \int_{-b/2}^{b/2} (x-x')\cos\frac{\pi y'}{b} \frac{e^{-j(kr+k_g\sqrt{x'^2+R'^2})}}{r^2} dx'dy' + \int_{-a/2}^{a/2} \int_{-b/2}^{b/2} (x-x')\cos\frac{\pi y'}{b} \frac{e^{-j(kr+k_g\sqrt{x'^2+R'^2})}}{r^3} dx'dy'\right] \quad . \tag{9}$$

The first integral in the brackets is proportional to $1/r^2$ while the second is proportional to $1/r^3$. Hence, for an approximation to the far fields of the horn, we neglect the second integral.

The analysis was previously restricted to the calculation of the fields on the ground plane only. It is, therefore, possible to approximate r for far field calculations by the relation

$$r=R-\frac{x}{R}x'-\frac{y}{R}y' = R-px'-qy'$$

where

$$p = \frac{x}{R} = \cos\phi$$

$$q = \frac{y}{R} = \sin\phi \ .$$

Applying the above indicated approximations to (9) and substituting the result into equation (2), produces the following expression for the electric field on the ground plane.

$$E_z = -j\omega\mu\,(\nabla x\,\pi_y^*\,\hat{y})_z$$

$$E_z = -\frac{jkE_o\,e^{-jkR}}{2\pi R^2}\int_{-a/2}^{a/2}\int_{-b/2}^{b/2}(x-x')\cos\frac{\pi y'}{b}\,e^{j(kpx'+kqy'-k_g\sqrt{x'^2+R'^2})}\,dx'dy'$$

$$=-\frac{jkE_oe^{-jkR}}{2\pi R}\int_{-b/2}^{b/2}\cos\frac{\pi y'}{b}e^{jkqy'}dy'\int_{-a/2}^{a/2}\frac{(x-x')}{R}e^{j(kpx'-k_g\sqrt{x'^2+R'^2})}\,dx'$$

$$E_z=-\frac{\hat{z}jkE_oe^{-jkR}}{2\pi R}\,I_1I_2 \ , \qquad (10)$$

where

I_1 = integral over y', and I_2 = integral over x' .

I_1 may be integrated in a straightforward manner to give

$$I_1 = \frac{b}{2}\left[\frac{\sin\left(\frac{kb}{2}\sin\phi+\frac{\pi}{2}\right)}{\left(\frac{kb}{2}\sin\phi+\frac{\pi}{2}\right)} + \frac{\sin\left(\frac{kb}{2}\sin\phi-\frac{\pi}{2}\right)}{\left(\frac{kb}{2}\sin\phi-\frac{\pi}{2}\right)}\right] . \tag{11}$$

A method for integrating I_2 in an exact manner was not available. Therefore, the integration was performed on the IBM 7090 computer.

Equation (10) is an expression for the far electric field on the ground plane produced by the E-sectoral horn. The resulting component of Poynting vector along the ground plane is

$$N(\phi) = \frac{1}{2}\sqrt{\frac{\epsilon}{\mu}}\left|E_z\right|^2 = \frac{1}{2}\left|\frac{-E_o kj\, e^{-jkR}}{2\pi R} I_1(\phi) I_2(\phi)\right|^2$$

$$= \sqrt{\frac{\epsilon}{\mu}}\left(\frac{E_o k}{8\pi R}\right)^2 \left|I_1(\phi)\right|^2 \left|I_2(\phi)\right|^2 . \tag{12}$$

The directivity of the horn for any direction ϕ along the ground plane may be obtained from the expression

$$D(\phi) = \frac{N(\phi)(4\pi R^2/2)}{W} = \frac{N(\phi)(2\pi R^2)}{W} \tag{13}$$

where

W = total power radiated from the antenna.

A computation of W could be performed by solving for the Poynting vector at all positions on a large hemispherical surface centered at the origin and then integrating it over that surface. Several alternative methods may be used to find an approximation expression for W.

A method which has been found to be satisfactory for present purposes is to integrate the Poynting vector over a constant phase wave front at the horn aperture. The Poynting vector on the cylindrical surface, defined in Fig. 2 by R'', $-\theta_o<\theta'<\theta_o$, and $-\frac{b}{2}<y'<\frac{b}{2}$, is

$$N = \frac{1}{2}\sqrt{\frac{\epsilon}{\mu}}\left|E_\theta\right|^2 = \frac{1}{2}\sqrt{\frac{\epsilon}{\mu}}E_o^2\cos^2\frac{2\pi y'}{b} .$$

Hence, the total power radiated is given by

$$W = \int\int_S NR''d\theta'dy' = \frac{1}{2}\sqrt{\frac{\epsilon}{\mu}}\,E_o^2R''\int_{-b/2}^{b/2}\int_{-\theta_o}^{\theta_o}\cos^2\frac{\pi y'}{b}d\theta'dy' .$$

The integrations may be performed in a straightforward manner, giving

$$W = \frac{\theta_o\sqrt{\frac{\epsilon}{\mu}}\,E_o^2R''b}{2} .$$

With the directivity defined in (13) the power coupling between two such horns mounted in the common ground plane is

$$C_{12} = \frac{D(\phi_1)D(\phi_2)\lambda^2}{(4\pi R)^2} = \frac{N(\phi_1)N(\phi_2)R^2\lambda^2}{4W^2} , \qquad (14)$$

where ϕ_1 and ϕ_2 are the orientation angles of the transmitting and receiving horns. Thus, by using (14), the coupling vs orientation pattern may be obtained theoretically.

A comparison of experimental and theoretical E-plane coupling curves for a pair of these horns operating at 10 Gc is shown in Fig. 3. The horns are fed with X-band wave guide and have a flare angle of 23^o. The aperture is 0.9x3.23 inches, and the center-to-center spacing between antennas is 14.5 inches.

These curves compare favorably in many respects. The only major deviations are in the relative depths of the nulls. The nulls in the experimental curve are not as deep as the corresponding nulls in the theoretical pattern. This result may be attributed to neglecting all but far field terms in the analysis.

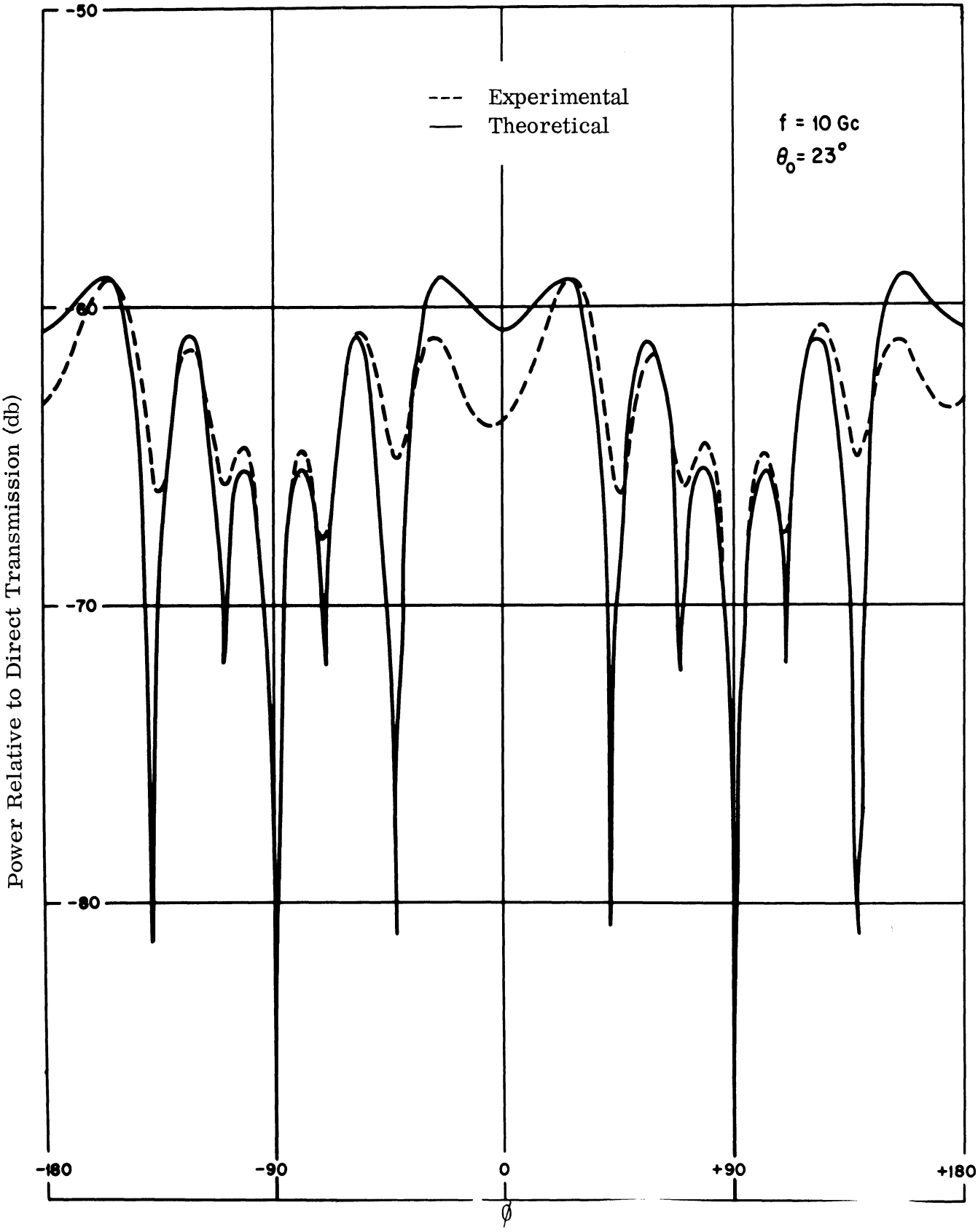

FIG. 3: E-SECTORAL HORN COUPLING

Additional coupling patterns were calculated for E-sectoral horns with the same aperture size (.9x3.23") and spacing but with different flare angles. These patterns are shown in Figs. 4a through 4d. It should be noted that the lobes on either side of the positions $\phi = \pm 90^o$ become smaller as the flare angle increases. For a flare angle of 40^o these lobes have vanished altogether. It is also interesting that maximum coupling does not occur when $\phi = 0^o$ but instead, when $\phi = \pm 24^o$. These patterns also indicate the positions of many nulls. These nulls may prove useful to decouple the antennas.

At present, mechanical devices are being built and tested which will permit experimental checks of the validity of the theoretical model for a variety of horn design parameters.

2.2 H-Sectoral Horns

The far field coupling between H-sectoral horns was derived in a manner similar to that used for the E-sectoral horns. The aperture field distribution was assumed to be

$$E_y = E_o \cos \frac{\pi x'}{a} e^{-jk\sqrt{x'^2+R'^2}}$$

where k is the free space propagation factor and the other parameters are defined in Fig. 5. The resulting far field expression for the electric field on the ground plane is

$$E_z = -\frac{jE_o e^{-jkR}}{2\pi R} \int_{-a/2}^{a/2} \cos\frac{\pi x'}{a} e^{j(kpx' - k\sqrt{x'^2+R'^2})} dx \int_{-b/2}^{b/2} \frac{k(y-y')}{R} e^{jkqy'} dy'$$

$$= -\frac{jE_o e^{-jkR}}{2\pi R} I_1 I_2 \quad ,$$

$p = \frac{x}{R} = \cos\phi$; $q = \frac{y}{R} = \sin\phi$; I_1 = integral over x', and I_2 = integral over y'.

I_2 may be integrated easily. The result is

$$I_2 = \frac{ky}{2}\left(\frac{2}{kq}\sin\frac{kqb}{2}\right) - \frac{1}{jRq}\left(b\cos\frac{kqb}{2} - \frac{2}{kq}\sin\frac{kqb}{2}\right) \quad .$$

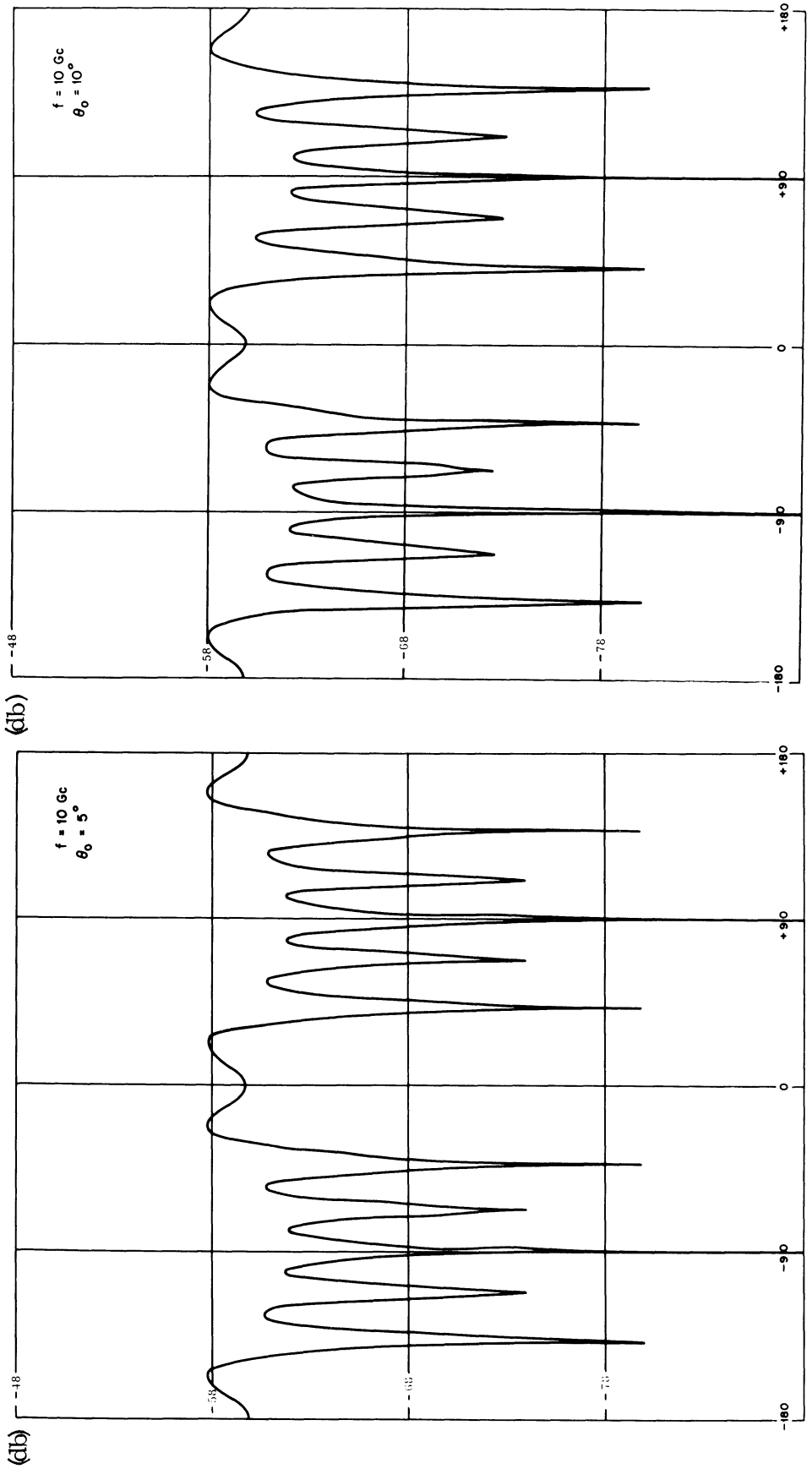

FIGS. 4a-4b: THEORETICAL E-PLANE COUPLING PATTERNS FOR E-SECTORAL HORNS

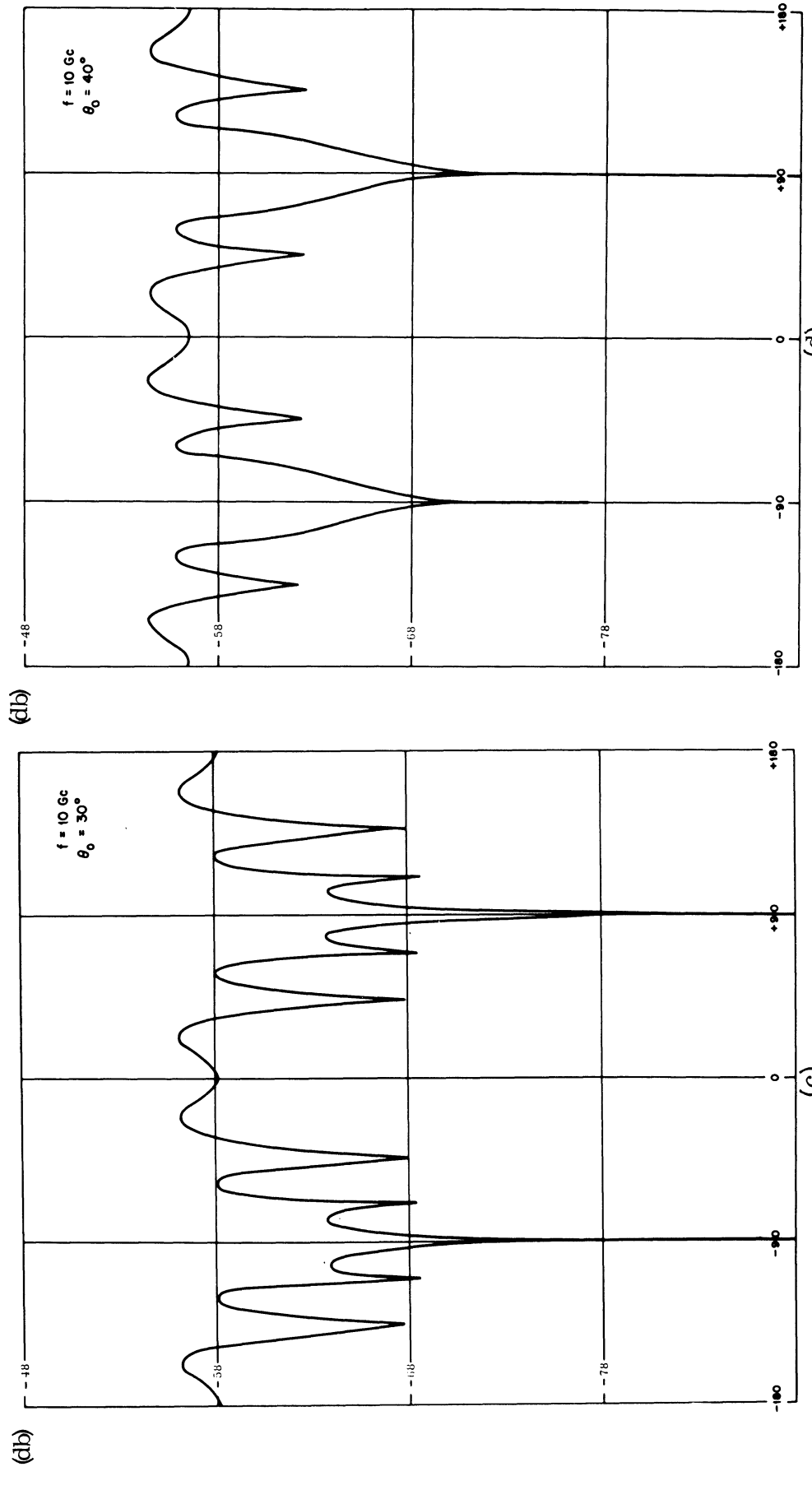

FIGS. 4c-4d: THEORETICAL E-PLANE COUPLING PATTERNS FOR E-SECTORAL HORNS

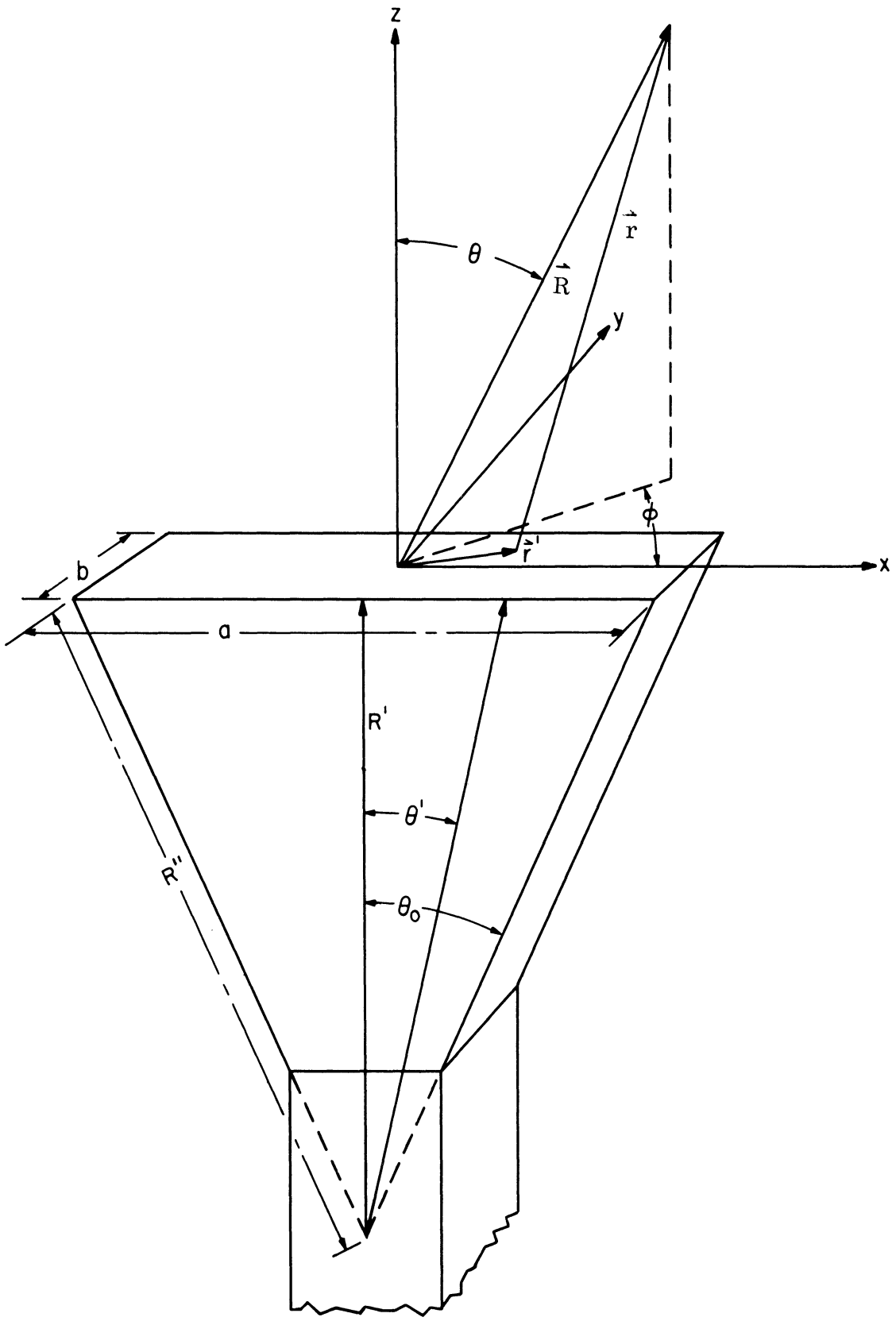

FIG. 5: H-SECTORAL HORN GEOMETRY

The computer was used to calculate I_1.

The resulting Poynting vector for the ϕ direction along the ground plane is

$$N(\phi)= \frac{1}{2}\sqrt{\frac{\epsilon}{\mu}}\left|E_z\right|^2 = \frac{1}{2}\sqrt{\frac{\epsilon}{\mu}}\left|\frac{jE_o e^{-jkR}}{2\pi R} I_1(\phi)I_2(\phi)\right|^2 = \sqrt{\frac{\epsilon}{\mu}}\left(\frac{E_o}{8\pi r}\right)^2 \left|I_1(\phi)\right|^2\left|I_2(\phi)\right|^2 . \quad (15)$$

An approximate value for W, the total power radiated, was calculated in a manner similar to that used for the E-sectoral horn. Referring to Fig. 5, the Poynting vector on the constant phase surface at the horn aperture was approximated by

$$N= \frac{1}{2}\sqrt{\frac{\epsilon}{\mu}}\left|E_y\right|^2 = \frac{1}{2}\sqrt{\frac{\epsilon}{\mu}}\, E_o^2 \cos^2\left(\frac{\pi\theta'}{2\theta_o}\right) .$$

Thus, W becomes

$$W= \int_S\int NR''d\theta'dy' = \frac{1}{2}\sqrt{\frac{\epsilon}{\mu}}\, R''E_o^2 \int_{-b/2}^{b/2}\int_{-\theta_o}^{\theta_o} \cos^2\left(\frac{\pi\theta'}{2\theta_o}\right)d\theta'dy'$$

$$= \frac{b\theta_o R''E_o^2}{2}\sqrt{\frac{\epsilon}{\mu}} . \quad (16)$$

Equations (15) and (16) may be used in (13) and (14) to calculate the directivity and power coupling for H-sectoral antennas.

A comparison of theoretical and experimental E-plane coupling patterns for two H-sectoral horns is shown in Fig. 6. The horns used have an aperture size of 0.4x3.25 inches and a flare angle of $\theta_o=33^o$. The center-to-center spacing is 14.5" and the frequency is 10 Gc. These patterns compare favorably in many respects. The coupling levels are comparable and the general shapes of the patterns are similar. Unlike the E-sectoral horn, this horn is flared in the plane of the H-field. Hence, it is possible for the higher order TE_{no} modes to exist at the aperture. The presence of one or more of these modes could account for the widening of the experimental pattern below the -50 db level as shown in Fig. 6. The effects of higher order modes will be studied in future work.

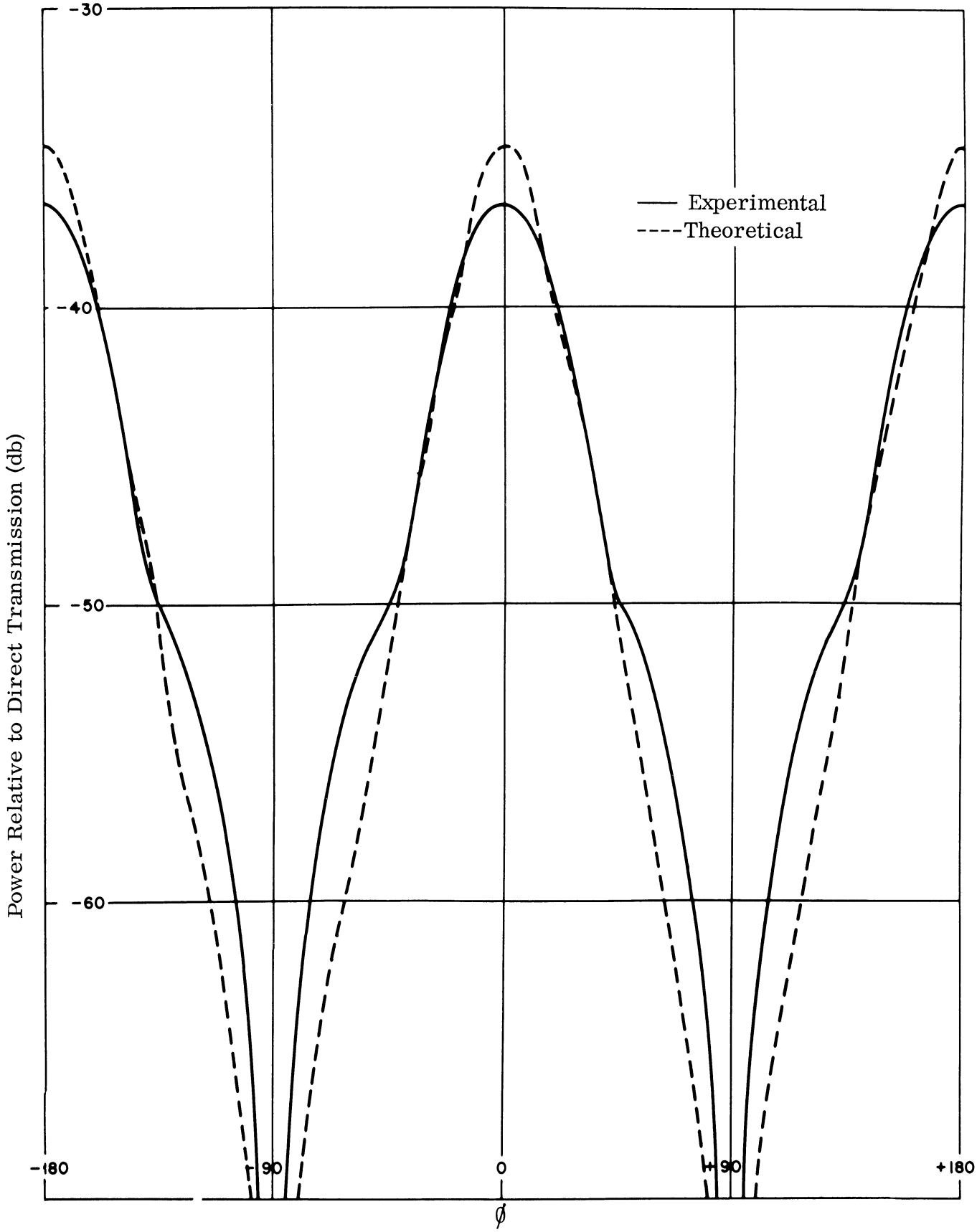

FIG 6: THEORETICAL AND EXPERIMENTAL H-SECTORAL HORN COUPLING PATTERNS.

2.3 Conical Horns

For the conical horn a theoretical derivation of the far-field coupling can be made. By postulating a tangential E-field, E_ρ and E_ϕ in the aperture of the conical horn, we can derive the Hertzian magnetic vector as :

$$\bar{\pi}^*(\bar{R}) = \frac{1}{2\pi j\omega\mu} \iint \left[\bar{E}(\bar{\rho}') \times \hat{n}\right] \frac{e^{-jk\left|\bar{R}-\bar{\rho}'\right|}}{\left|\bar{R}-\bar{\rho}'\right|} dA' \quad . \tag{17}$$

The factor in front of the integral already includes the imaging effect of the ground plane. $\bar{E} \times \hat{n}$, the tangential E-field, vanishes in the ground plane. Therefore, the only contribution to the integral comes from the horn aperture.

From the Hertzian magnetic vector, we can obtain the fields as:

$$\bar{E} = -j\omega\mu \nabla \times \bar{\pi}^* \tag{18}$$

$$\bar{H} = \nabla(\nabla \cdot \bar{\pi}^*) + k^2 \bar{\pi}^* \quad . \tag{19}$$

Using a spherical coordinate system as indicated in Fig. 7, in the ground plane ($\theta = \pi/2$) we will have only E_θ nonvanishing. The field component E_θ is given by (Silver, 1949),

$$E_\theta(\theta=\pi/2) = \frac{jke^{-jkR}}{2\pi R} \left[N_x \cos\phi + N_y \sin\phi\right] \tag{20}$$

where N_x and N_y represent the integrals in $\bar{\pi}_x^*$ and $\bar{\pi}_y^*$:

$$N_x = \iint (E_t)_x e^{jk(x'\cos\phi + y\sin\phi)} dA' \tag{21}$$

$$N_y = \iint (E_t)_y e^{jk(x'\cos\phi + y'\sin\phi)} dA' \quad . \tag{22}$$

Everywhere primed coordinates designate variables in the source aperture and unprimed coordinates, those at a field point. Using the relations $x' = \rho'\cos\phi'$, $y' = \rho'\sin\phi'$ (see Fig. 8), we get:

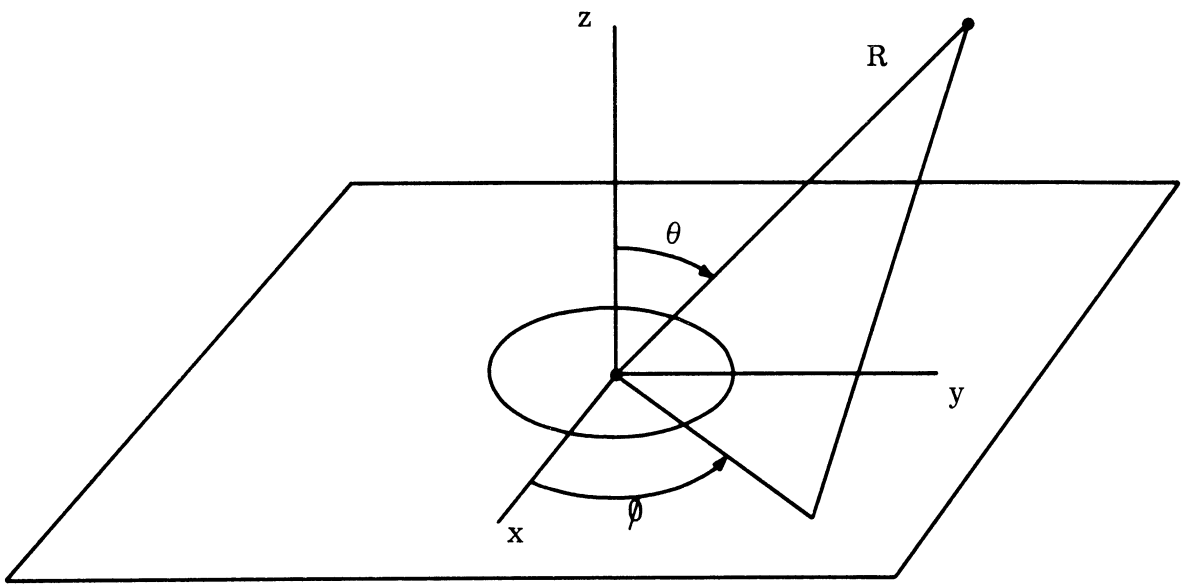

FIG. 7: COORDINATE SYSTEM FOR CONICAL HORN

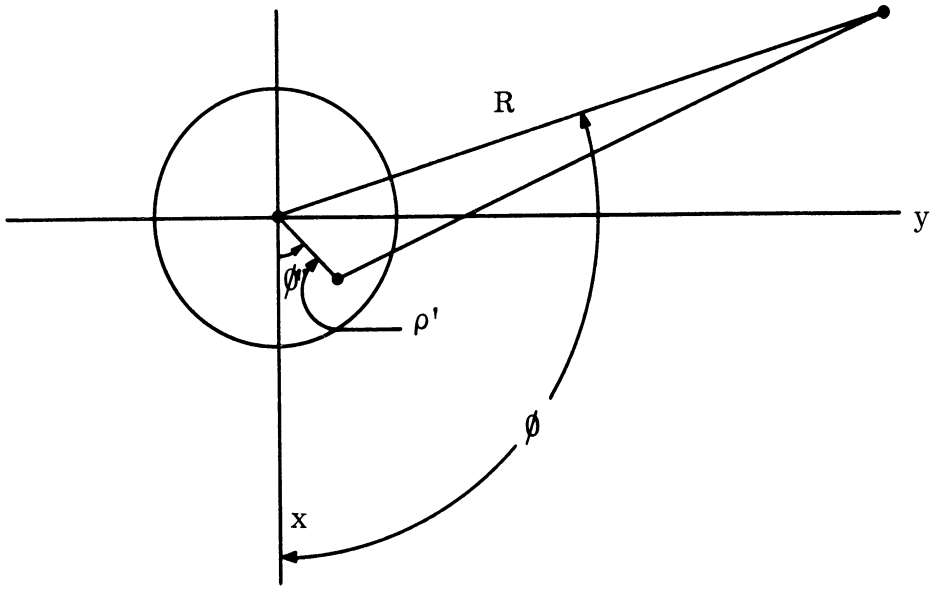

FIG. 8: COORDINATE SYSTEM IN GROUND PLANE FOR CONICAL HORNS

$$N_x = \iint (E_t)_x e^{jk\rho'\cos(\phi-\phi')} \rho' d\rho' d\phi' \tag{23}$$

$$N_y = \iint (E_t)_y e^{jk\rho'\cos(\phi-\phi')} \rho' d\rho' d\phi' \quad . \tag{24}$$

In order to evaluate the far field pattern, the tangential aperture field $\bar{E}_t$ has to be derived or postulated. For the present case, it was assumed that in the aperture the tangential E-field could be represented as a combination of circular waveguide modes TE_{11} and TM_{11}, both of them having their phase centers at the point where the extended walls of the conical horn would intersect (see Fig. 9). There is experimental evidence available (Potter, 1963) that a mixture of these two modes actually exists in the aperture of even moderate flare angle conical horns.

The aperture fields assumed to exist are given by:

TE_{11}:

$$E_{\rho'} = \frac{j\omega\mu K'_{11} F \sin\phi' J_1(K'_{11}\rho')}{K'_{11}\rho'} \tag{25}$$

$$E_{\phi'} = -j\omega\mu K'_{11} F \cos\phi' J'_1(K'_{11}\rho') \tag{26}$$

where

$$F = \exp\left[-j \frac{2\pi}{\lambda}\sqrt{L^2+\rho'^2}\right] , \tag{27}$$

(for the definition of L, see Fig. 9), and where $(K'_{11}a)$ is the first root of J'_1;

$$J'_1(K'_{11}a) = 0 \tag{28}$$

TM_{11}:

$$E_{\rho'} = 2j\omega\mu K'_{11} F \sin\phi' J_1(K_{11}\rho') \tag{29}$$

$$E_{\phi'} = \frac{2j\omega\mu K'_{11} F \cos\phi' J_1(K'_{11}\rho')}{K_{11}\rho'} , \tag{30}$$

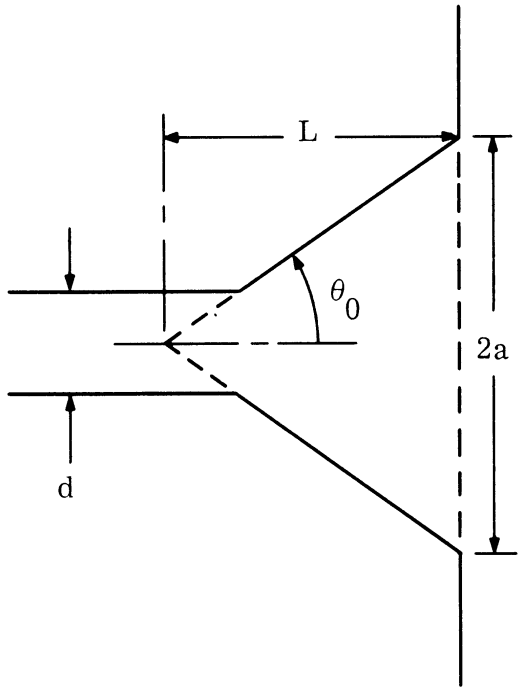

FIG. 9: CROSS SECTIONAL VIEW OF CONICAL HORN
a = 4.6cm, d=2.54cm, L=26.4cm, θ_o=9.9°.

where $(K_{11}a)$ is defined as the first zero of

$$J_1(K_{11}a) = 0; \tag{31}$$

and F is defined above. In order to evaluate N_x and N_y (eqns. 23 and 24), we have to decompose the aperture fields into their rectangular components, giving:

TE_{11}:

$$E_{x'} = \frac{1}{2} j\omega\mu K'_{11} F \left[J_2(K'_{11}\rho')\sin 2\phi'\right] \tag{32}$$

$$E_{\phi'} = 2j\omega\mu K'_{11} F \left[J_o(K'_{11}\rho') - J_2(K'_{11}\rho')\cos 2\phi'\right] \tag{33}$$

TM_{11}:

$$E_{x'} = -j\omega\mu K_{11} F J_2(K_{11}\rho')\sin 2\phi' \tag{34}$$

$$E_{y'} = j\omega\mu K_{11} F \left[J_o(K_{11}\rho') + J_2(K_{11}\rho')\cos 2\phi'\right] . \tag{35}$$

For the TE_{11} mode we obtain:

$$N_x = +A \iint F \sin\phi' e^{jk\rho'\cos(\phi-\phi')} J_2(K'_{11}\rho')\rho' d\rho' d\phi' \tag{36}$$

$$N_y = A \iint F\left[J_o(K'_{11}\rho') - J_2(K'_{11}\rho')\cos 2\phi'\right] e^{jk\rho'\cos(\phi-\phi')} \rho' d\rho' d\phi' \tag{37}$$

where

$$A = \frac{1}{2} j\omega\mu K_{11} .$$

Using the expansion

$$e^{jx\cos y} = J_o(x) + \sum_{n=1}^{\infty} 2j^n J_n(x)\cos ny , \tag{38}$$

these become:

$$N_x = -2\pi A \sin 2\phi \, \Gamma_2(K'_{11}) \tag{39}$$

$$N_y = 2\pi A \left[\Gamma_0(K'_{11}) + \Gamma_2(K'_{11})\cos 2\phi\right] \tag{40}$$

where

$$\Gamma_o(\gamma) = \int_o^a F\rho' J_o(\gamma\rho') J_o(k\rho') d\rho' \tag{41}$$

$$\Gamma_2(\gamma)=\int_o^a F\rho' J_2(\gamma\rho')J_2(k\rho')d\rho' \quad . \tag{42}$$

For the TM_{11} mode we obtain

$$N_x=-2A\iint F\sin 2\phi' e^{jk\rho'\cos(\phi-\phi')} J_2(K_{11}\rho')\rho' d\rho' d\phi' \tag{43}$$

$$N_y=2A\iint F\left[J_o(K_{11}\rho')+J_2(K_{11}\rho')\cos 2\phi'\right] e^{jk\rho'\cos(\phi-\phi')}\rho' d\rho' d\phi' \quad , \tag{44}$$

which becomes

$$N_x=4\pi A\sin 2\phi\,\Gamma_2(K_{11}) \tag{45}$$

$$N_y=4\pi A\left[\Gamma_o(K_{11})-\Gamma_2(K_{11})\cos 2\phi\right] \quad . \tag{46}$$

Combining the contributions due to the x and y polarizations according to (20), we have

$$E_{\theta TE_{11}}=\frac{jkA}{R}\left[\Gamma_o(K'_{11})-\Gamma_2(K'_{11})\right]\sin\phi \tag{47}$$

$$E_{\theta TM_{11}}=\frac{2jkA}{R}\left[\Gamma_o(K_{11})+\Gamma_2(K_{11})\right]\sin\phi \tag{48}$$

or, equivalently,

$$E_{\theta TE_{11}}=\frac{\omega\mu K'_{11}k}{R}\left[\Gamma_o(K'_{11})-\Gamma_2(K'_{11})\right]\sin\phi \tag{49}$$

$$E_{\theta TM_{11}}=\frac{2\omega\mu K'_{11}k}{R}\left[\Gamma_o(K'_{11})+\Gamma_2(K'_{11})\right]\sin\phi \quad . \tag{50}$$

The integrals Γ_o and Γ_2 (eqns. 41 and 42) cannot be evaluated in closed form because of the factor F. However, in the limiting case of an aperture fed by a circular waveguide of the same size, this factor becomes equal to one. In this case Γ_o and Γ_2 can be evaluated exactly using the relationship (Silver, 1949);

$$\int_o^a y J_n(\alpha y)J_n(\beta y)dy=\frac{a}{\alpha^2-\beta^2}\left[J_n(\alpha a)\beta J'_n(\beta a)-J_n(\beta a)\alpha J'_n(\alpha a)\right] \quad . \tag{51}$$

Now, using the boundary condition $J_1'(K_{11}a)=0$ for the TE_{11} mode, and $J_1(K_{11}a)=0$ for the TM_{11} mode, we finally derive:

$$\Gamma_o(K_{11}')= \frac{a}{K_{11}'^2-k^2} J_o(K_{11}'a)\left[K_{11}'^2 aJ_o(ka)-kJ_1(ka)\right] \tag{52}$$

$$\Gamma_2(K_{11}')= \frac{a}{K_{11}'^2-k^2} J_o(K_{11}'a)\left[kJ_1(ka)-K_{11}'^2 aJ_2(ka)\right] \tag{53}$$

$$\Gamma_o(K_{11}')= \frac{-ka}{K_{11}'^2-k^2} J_o(K_{11}'a)J_1(ka) \tag{54}$$

$$\Gamma_2(K_{11}')=- \frac{ka}{K_{11}'^2-k^2} J_o(K_{11}'a)J_1(ka) \quad . \tag{55}$$

Therefore, the particular combinations we need for deriving the normal E-field, equations (49) and (50), are:

$$\Gamma_o(K_{11}')-\Gamma_2(K_{11}')= \frac{2a}{k} J_o(K_{11}'a)J_1(ka) \tag{56}$$

$$\Gamma_o(K_{11})+\Gamma_2(K_{11})= - \frac{2ka}{K_{11}^2-k^2} J_o(K_{11}a)J_1(ka) \quad . \tag{57}$$

The directivity of an antenna is given as

$$D(\phi)= \frac{P(\phi)2\pi R^2}{W} \quad , \tag{58}$$

where $P(\phi)$ is the power density in the ϕ-direction, and W is the total radiated power by the transmitting antenna. Then,

$$D = \frac{\frac{1}{2}\sqrt{\frac{\epsilon}{\mu}}\left|E_\theta\right|^2 2\pi R^2}{W} \quad . \tag{59}$$

To calculate W, evaluate $\frac{1}{2}\,\mathrm{Re}(E_t \times H_t^*)$ over the aperture, giving:

$$W = \frac{k}{2\omega\mu}\int_o^{2\pi}\int_o^a \left(\left|E_x\right|^2+\left|E_y\right|^2\right)\rho' d\rho' d\phi' \quad . \tag{60}$$

There results for the TE_{11} and TM_{11} modes, respectively:

$$W_{TE_{11}} = \frac{\pi \beta'_{11} K'^2_{11} \omega\mu}{4} \int_0^a \left[J_o^2(K'_{11}\rho') + J_2^2(K'_{11}\rho') \right] \rho' d\rho'$$

$$= \frac{\pi \beta_{11} \omega\mu}{4} (K'^2_{11} a^2 - 1) J_1^2 (K'_{11} a) \tag{61}$$

where

$$\beta_{11} = \sqrt{k^2 - K'^2_{11}} \tag{62}$$

$$W_{TM_{11}} = 16 \pi \omega\mu \frac{k^2 K_{11}^2}{\beta'_{11} \beta_{11}} J_o^2 (K_{11} a) \tag{63}$$

where

$$\beta'_{11} = \sqrt{k^2 - K_{11}^2} \ . \tag{64}$$

The total radiated power by the conical horn then will be the sum of that contained in the TE_{11} and TM_{11} modes, i. e.

$$W_{total} = R_1^2 W_{TE_{11}} + R_2^2 W_{TM_{11}} \ , \tag{65}$$

where R_1 and R_2 are the amplitudes with which the TE_{11} and TM_{11} modes are excited, respectively .

Using the directivity of the conical horn, we can derive the coupling by the formula:

$$C = \frac{D_1 D_2 \lambda^2}{4\pi R^2} \ , \tag{66}$$

where

D_1 = directivity of transmitting horn in the direction of the receiving horn,

D_2 = directivity of the receiving horn in the direction of the transmitting horn .

Now, for identical transmitting and receiving horns,

$$D = D_1 = D_2 \tag{67}$$

and the coupling becomes

$$C = \frac{D^2\lambda^2}{4\pi R^2} \quad . \tag{68}$$

While we can derive a closed form expression for F=1 for Γ_o and Γ_2 (equations 41 and 42), these equations can be evaluated very easily numerically for any F. A computer program was written for this purpose, evaluating the integrals by using Simpson's formula. A thorough study of the effects of having present both the TE_{11} mode and the TM_{11} mode is under way. Figure 10 shows the theoretical maximum coupling value obtained as a function of frequency with a pair of horns of radius a=4.6 cm, center-to-center spacing 36.6 cm, and length L=26.4 cm, R_1=.9, R_2=.1 . Only a plot of the maximum coupling is needed in order to deduce the coupling for any orientation of the conical horns, since the directivity in the ground plane varies as $\sin\phi$.

2.4 General Analysis of Sectoral Horn Coupling

A horn excited by a waveguide supporting a TE_{10} mode is to be considered. Inside the horn the TE_{10} mode from the waveguide will be decomposed into an infinite number of modes compatible with the geometry of the horn. If the length of the horn is sufficiently large, the pseudo TE_{10} mode will be dominant in the region far from A and B (see Fig. 11). Similar observations can be made with a receiving horn and its associated structures.

The legitimate approach to this problem is, of course, to match the coefficients of modes in each of the five regions (Fig. 11) in terms of the incident TE_{10} mode. The difficulties in this approach arise due to the fact that the geometry of a horn is not orthogonal in Cartesian coordinate systems . In other words, it is impossible to find one coordinate system which preserves the orthogonality in all regions, thus leading to the infinite mode transmission matrix. When flare angles of the horn are

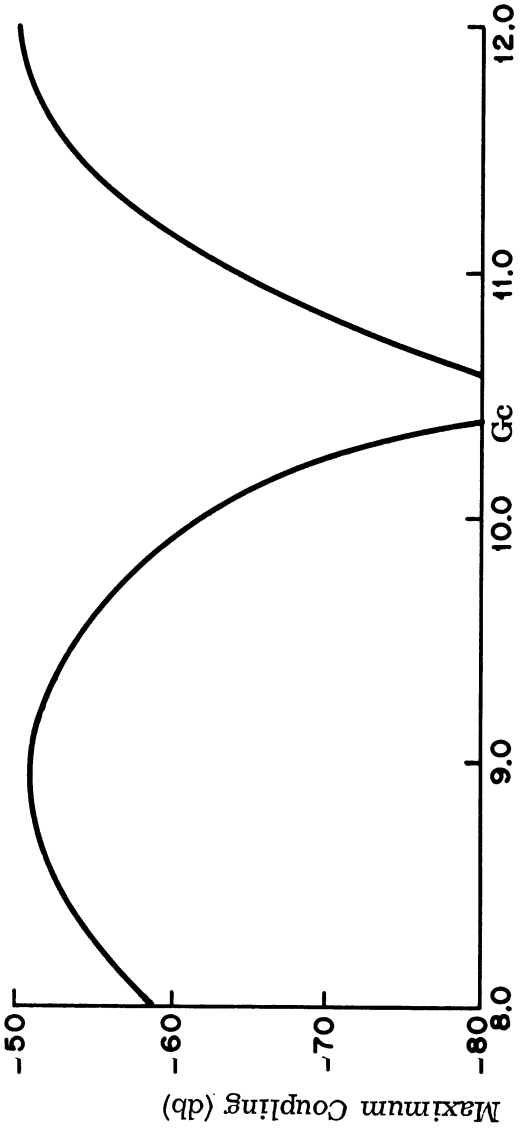

FIG. 10: COMPUTED COUPLING LEVELS FOR CONICAL HORNS AS A FUNCTION OF FREQUENCY. R_1=.9, R_2=.1, a=4.6cm, s= center-to-center spacing=36.6cm.

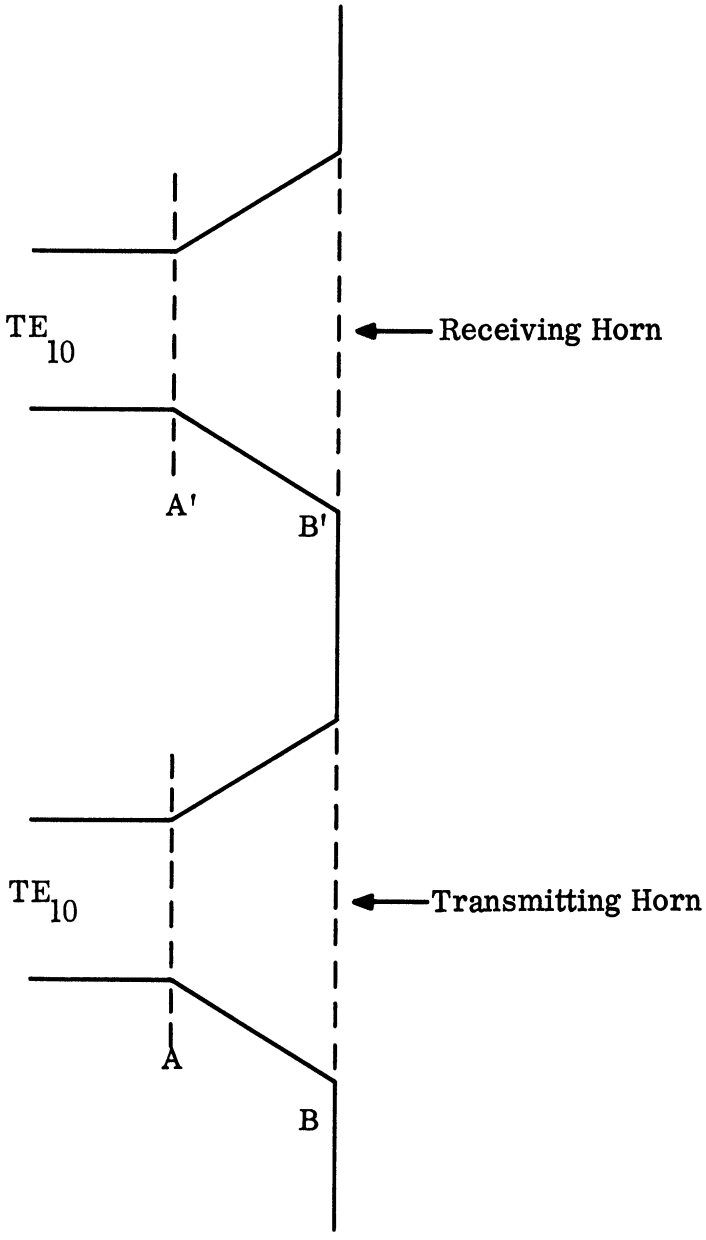

FIG. 11: CONFIGURATION OF TWO HORN SYSTEMS

small, the modes in the horn can be approximated in terms of the Cartesian coordinate system by using WKB methods. Even in this case, the amount of calculation is enormous.

To avoid these difficulties, it is assumed that the aperture field of the horn consists only of the pseudo TE_{10} mode, thus eliminating the necessity of considering many characteristics of waveguide and horn structures. In addition to the above, the following will be assumed.

1) No reflection occurs at A and A'.
2) Aperture field over the transmitting horn has the same distribution as the dominant mode in the horn.
3) Secondary scattering effects will be ignored.

The above approach is merely the extension of analysis of the coupling of waveguide terminated slot antennas. Therefore, in the subsequent analysis many steps will be omitted as they have already been reported.

As in the Introduction, a few words seem to be in order about the relations between the present approach and the coupling formula using directivity concepts which have been treated in earlier sections. Generally, the directivity has a meaning only in the region far from the source where the field intensity is proportional to $1/r$. The usefulness of the directivity ceases if the field intensity is proportional to $1/r^2$ or the far field component is comparable to the near field component. The present approach has, as one of its objectives, to seek a unified form which is applicable both in the near and far regions.

The two-horn system, flush mounted in the perfectly conducting plane, is shown in Fig. 12. The system A is transmitting and B is receiving. The orientation of B with respect to A is arbitrary. For computational convenience the sizes of two systems are assumed to be identical. The coordinate systems with reference to the centers of the Horn A and horn B are (ξ, η, ζ) and (x, y, z) respectively. The relation

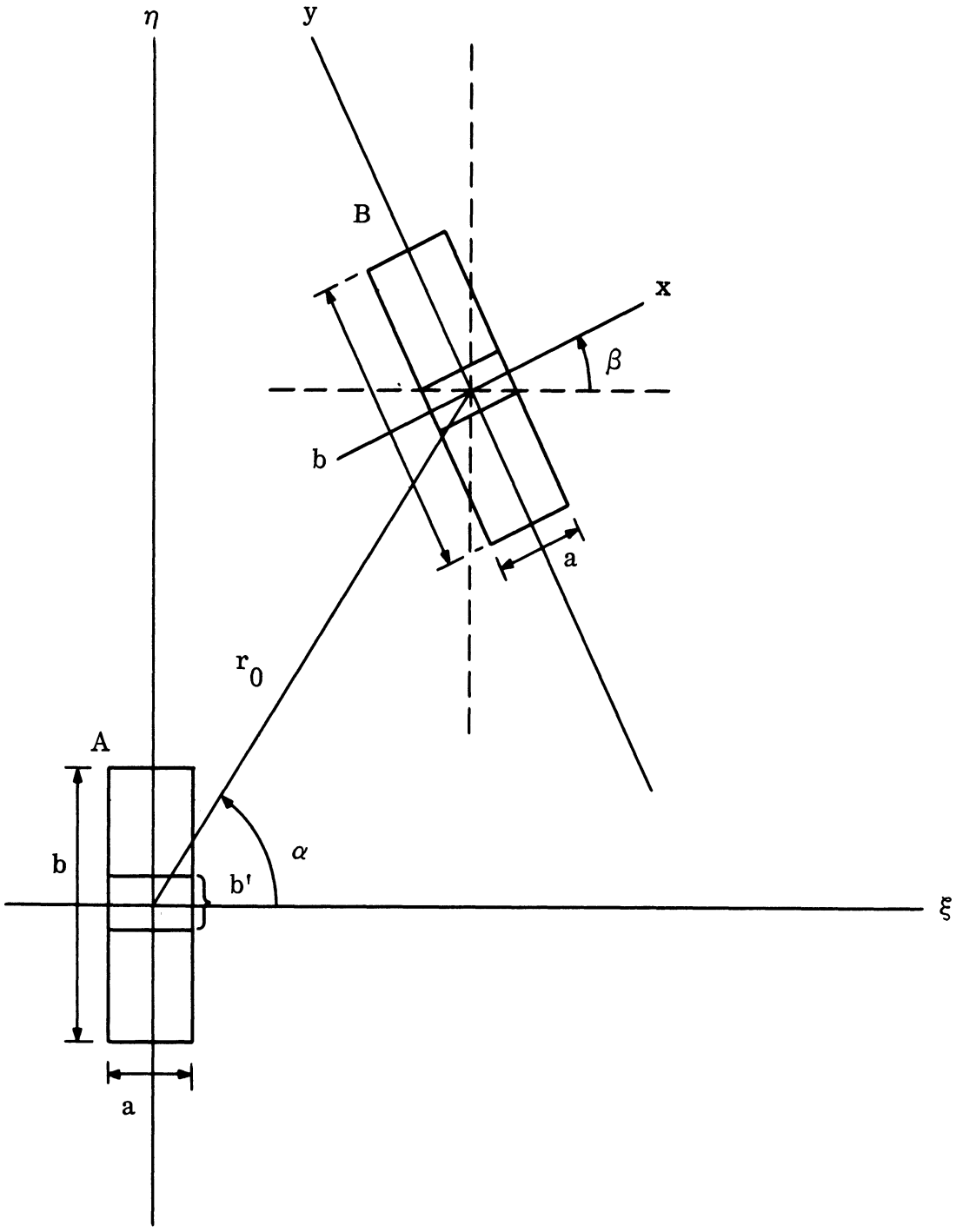

FIG. 12: COORDINATE SYSTEM OF TWO HORNS

between (ξ, η, ζ) and (x, y, z) is

$$\begin{aligned} \xi &= r_o \cos\alpha + x\cos\beta - y\sin\beta \\ \eta &= r_o \sin\alpha + x\sin\beta + y\cos\beta \\ \zeta &= z \quad . \end{aligned} \tag{69}$$

The coordinate system is shown in Fig. 13. The point 0 is located at the middle of the intersection line of the flared sides.

The coupling C is defined as

$$C = W_r/W_t \quad , \tag{70}$$

where W_r is the power received by the receiving system and W_t is the power transmitted. The analysis of coupling consists, therefore, in the calculation of W_r and W_t.

First, field intensities in the half-space will be calculated. When the receiving horn is covered by a perfectly conducting thin sheet, the magnetic field H_0 in the half-space can be written in terms of the aperture field in the transmitting horn as follows:

$$\bar{H}_0(\bar{r}_A) = \int_A \int \bar{\bar{Y}}_n(\bar{r}_A, \bar{\rho}_A) \cdot \left[\bar{E}(\bar{\rho}_A) \times \zeta_o\right] dS_{A'} \tag{71}$$

where

$$\bar{\bar{Y}}_n(\bar{r}_A, \bar{\rho}_A) = \frac{1}{2\pi j\omega\mu} (k^2 \bar{\bar{I}} + \nabla\nabla) \frac{e^{-jk\left|\bar{r}_A - \bar{\rho}_A\right|}}{\left|\bar{r}_A - \bar{\rho}_A\right|} \tag{72}$$

$\bar{\rho}_A(\xi', \eta', \zeta')$ = source coordinate of the transmitting aperture,

$\bar{r}_A(\xi, \eta, \zeta)$ = position vector of the field point from the source point in A,

$\bar{\bar{I}}$ is the unit dyadic.

To calculate the field transmitted into the receiving horn, the following conditions on the boundary constraint will be made.

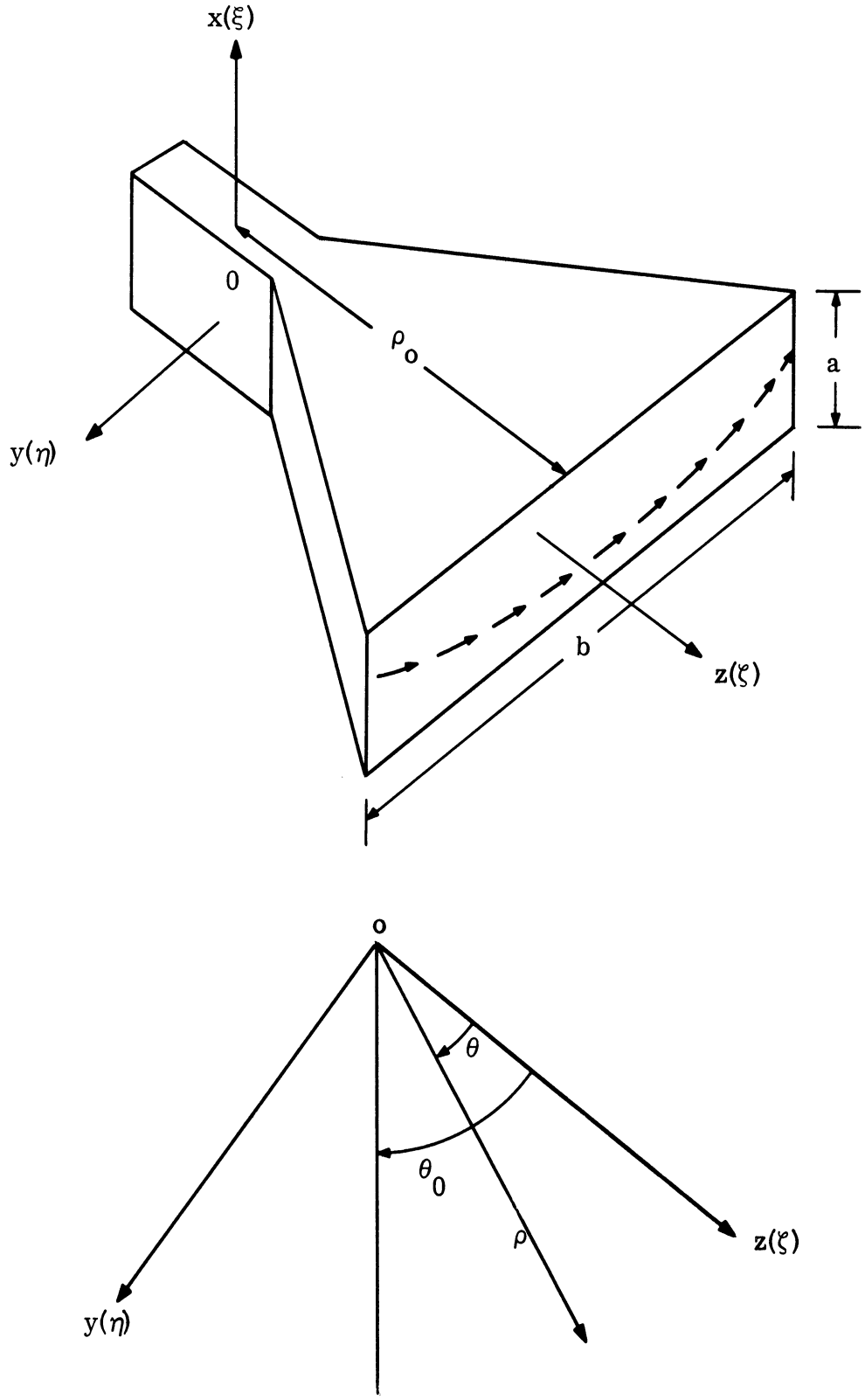

FIG. 13: HORN AND ITS COORDINATES

1) Ignore the presence of the transmitting system (i. e. the field over the transmitting system is fixed).

2) When the receiving aperture is covered with a conducting thin sheet, the fields satisfy the boundary conditions:

$$\bar{H}_0 = \bar{H}_{0t},\ \bar{H}_{0n} = 0 \qquad \text{at } z = 0$$

$$\bar{E}_0 = \bar{E}_{0n},\ \bar{E}_{0t} = 0 \qquad \text{at } z = 0 \tag{73}$$

where t and n indicate tangential and normal components respectively.

3) On removing the conductor, fields in the receiving horn satisfy the boundary conditions:

$$\bar{H}_{it} = \bar{H}_{0t} + \bar{H}_{0s} \qquad \text{at } z = 0$$

$$\bar{E}_{it} = \bar{E}_{0s} \qquad \text{at } z = 0 \tag{74}$$

where s denotes the tangential component of a scattered field. If the receiving horn were a uniform rectangular (or cylindrical) structure, $\bar{H}_{0s}$ would be equal to $(-\bar{H}_{it})$, thus leading to the relation:

$$\bar{H}_{it} = \frac{1}{2}\bar{H}_{0t} \quad . \tag{75}$$

In the case of actual horns, this relation does not hold. However, for the horn with a small flare angle, we adopt the above relation which is not unreasonable in view of the assumptions we have been making so far.

4) $\bar{H}_{it}$ thus obtained travels through the horn to the waveguide where only the dominant TE_{10} component has meaning as far as measurement of the received power is concerned. As already mentioned, it is assumed that the pseudo TE_{10} mode in the horn will be converted to the TE_{10} mode in the guide without any loss of power during the process of conversion. It is admitted that this is a very drastic assumption, but this seems to be the only way to avoid solving an infinite determinental characteristic equation.

In view of the above decisions or assumptions (1) through (4), and using equations (71) and (75), we obtain the amplitude I of the TE_{10} component in the following form:

$$I=\frac{1}{2}\int_B\int \bar{h}(x,y)\cdot \bar{\bar{H}}_0(\bar{\rho}_B)dS_B$$

$$=\frac{1}{2}\int_B\int dS_B\int_A\int dS_A \bar{h}(\bar{\rho}_B)\bar{\bar{Y}}_n(\bar{\rho}_A\bar{\rho}_B)\cdot\left[\bar{E}(\bar{\rho}_A)x\,\hat{\xi}_o\right] \quad , \tag{76}$$

where $\bar{h}(\bar{\rho}_B)=\bar{h}(x,y)$ is the normalized, transverse pseudo TE_{10} vector mode.

The determination of $\bar{E}(\bar{\rho}_A)$ involves an integral equation for which the exact solution is not available. To avoid this difficulty, as stated earlier, it is assumed that $\bar{E}(\bar{\rho}_A)$ can be represented approximately by the dominant pseudo TE_{10} mode of the transmitting horn. The pseudo TE_{10} mode is given as

$$H''_x= \gamma^2 H_0^{(2)}(\gamma\rho)\cos\frac{\pi x}{a}$$

$$H''_\rho= -\left(\frac{\pi}{a}\right)\frac{\partial}{\partial\rho}\left[H_0^{(2)}(\gamma\rho)\right]\sin\left(\frac{\pi x}{a}\right)$$

$$E''_\theta = j\omega\mu\frac{\partial}{\partial\rho}\left[H_0^{(2)}(\gamma\rho)\right]\cos\frac{\pi x}{a} \quad , \tag{77}$$

where

$$\gamma = \sqrt{k^2-\left(\frac{\pi}{a}\right)^2} \quad .$$

If $\gamma\rho \gg 1$, the above modes can be written as:

$$H''_x= \gamma^2\sqrt{\frac{2}{\pi\gamma\rho}}\,e^{-j\gamma\rho}\,e^{j\pi/4}\cos\frac{\pi x}{a}$$

$$H''_\rho= j\frac{\pi\gamma}{a}\sqrt{\frac{2}{\pi\gamma\rho}}\,e^{-j\gamma\rho}\,e^{j\pi/4}\cos\frac{\pi x}{a}$$

$$E''_\theta=\omega\mu\gamma\sqrt{\frac{2}{\pi\gamma\rho}}\,e^{-j\gamma\rho}\,e^{j\pi/4}\cos\frac{\pi x}{a} \quad . \tag{78}$$

These equations can also be written in terms of the Cartesian coordinates. The

transverse components in the x-y plane are:

$$H_x'' = \gamma^2\sqrt{\frac{2}{\pi\gamma}}\, e^{j\pi/4}\, \frac{e^{-j\gamma\sqrt{\rho_o^2+y^2}}}{(\rho_o^2+y^2)^{1/4}} \cos\frac{\pi x}{a}$$

$$H_y'' = j\frac{\pi\gamma}{a}\sqrt{\frac{2}{\pi\gamma}}\, e^{j\pi/4}\, \frac{y e^{-j\gamma\sqrt{\rho_o^2+\eta^2}}}{(\rho_o^2+\eta^2)^{3/4}} \sin\frac{\pi x}{a} \qquad (79)$$

$$E_y'' = -\omega\mu\gamma\sqrt{\frac{2}{\pi\gamma}}\, e^{j\pi/4}\, \frac{\rho_o e^{-j\gamma\sqrt{\rho_o^2+\eta^2}}}{(\rho_o^2+\eta^2)^{3/4}} \cos\frac{\pi x}{a} \quad .$$

If the flare angle of the horn is small, then

$$\cos\theta = \frac{\rho_o}{\sqrt{\rho_o^2+\eta^2}} \doteq 1$$

$$\sin\theta = \frac{\eta}{\sqrt{\rho_o^2+\eta^2}} \doteq \frac{\eta}{\rho_o}$$

$$(\rho_o^2+y^2)^{1/4} \doteq \rho_o^{1/2} \quad . \qquad (80)$$

Under this approximation (79) can be rewritten as

$$H_x'' = \gamma^2\sqrt{\frac{2}{\pi\gamma\rho_o}}\, e^{j\pi/4}\, e^{-j\gamma\sqrt{\rho_o^2+y^2}} \cos\frac{\pi x}{a}$$

$$H_y'' = j\frac{\pi\gamma}{a}\sqrt{\frac{2}{\pi\gamma\rho_o}}\, e^{j\pi/4} \cdot \frac{y}{\rho_o}\, e^{-j\gamma\sqrt{\rho_o^2+y^2}} \sin\frac{\pi x}{a} \qquad (81)$$

$$E_y'' = -\omega\mu\gamma\sqrt{\frac{2}{\pi\gamma\rho_o}}\, e^{j\pi/4}\, e^{-j\gamma\sqrt{\rho_o^2+y^2}} \cos\frac{\pi x}{a} \quad .$$

Identifying $E(\rho_A)=E''_\eta(\xi,\eta)$ and taking $\bar{h}$ as the normalized version of $\bar{H}=x_o H''_x + y_o H''_y$, the equation forms:

$$I_1 = -\frac{1}{2}\omega\mu\gamma\sqrt{\frac{2}{\pi\gamma\rho_o}}\,e^{j\pi/4}\,\frac{\iint dS_B \iint dS_A\left[\hat{x}_o H''^{*}_x + y_o H''^{*}_y\right]\cdot\bar{\bar{Y}}_n\cdot\hat{\xi}_o\, e^{-j\gamma\sqrt{\rho_o^2+\xi^2}}\cos\frac{\pi x}{a}}{\left[\iint\left|H''_x\right|^2 dS_B + \iint\left|H''_y\right|^2 dS_B\right]}$$

$$= \frac{\omega\mu\gamma}{\pi\rho_o}\,\frac{\iint dS_B \iint dS_A X(\eta)\,X^{*}(y)\left\{\hat{x}_o\,\gamma\cos\frac{\pi x}{a} - j\hat{y}_o\,\frac{\pi y}{a\rho_o}\sin\frac{\pi x}{a}\right\}\cdot\bar{\bar{Y}}_n\cdot\hat{\xi}_o\cos\frac{\pi x}{a}}{\left[\iint\left|H''_x\right|^2 dS_B + \iint\left|H''_y\right|^2 dS_B\right]}\,, \tag{82}$$

where

$$X(\eta) = e^{-j\gamma\sqrt{\rho_o^2+\eta^2}}\,. \tag{83}$$

If we can ignore H''_y compared with H''_x, (82) will take the form:

$$I = K_o\int_{-b/2}^{b/2} dy \int_{-b/2}^{b/2} d\eta\, X(\eta)X^{*}(y)J(\eta,y) \tag{84}$$

where

$$K_o = -\frac{1}{2jab\gamma} \tag{85}$$

$$J(\eta,y) = \int_{-a/2}^{a/2} dx \int_{-a/2}^{a/2} d\xi\cos\frac{\pi x}{a}\cos\frac{\pi\xi}{a}\hat{x}_o\cdot\left[k^2\bar{\bar{I}}+\nabla\nabla\right]\cdot\hat{\xi}_o\left(G(\bar{\rho}_B\bar{\rho}_A)\right) \tag{86}$$

$$G(\bar{\rho}_B\bar{\rho}_A) = \frac{e^{-jk\left|\bar{\rho}_B-\bar{\rho}_A\right|}}{\left|\rho_B-\rho_A\right|} = G(x,y\,|\,\xi,\eta)\,, \tag{87}$$

where $\bar{\rho}_B$ is the position vector over the receiving aperture in terms of the coordinate system (x, y, z) while $\bar{\rho}_A$ still keeps the meaning of equation (72). It is to be noted that the differentiation affects only $\bar{\rho}_B$.

At this point it should be mentioned that though the contribution of H_y'' to the coupling is usually small, this effect cannot be ignored when the near field is dominant. However, this contribution of H_y'' will not be dealt with in this report.

In view of equation (69) and Fig. 12;

$$\hat{x}_o \cdot (k^2 \bar{\bar{I}} + \nabla\nabla) \cdot \hat{\xi}_o = k^2 \cos\beta + \cos\beta \frac{\partial^2}{\partial x^2} - \sin\beta \frac{\partial}{\partial x} \frac{\partial}{\partial y} \quad . \tag{88}$$

The substitution of (88) into (86) leads to

$$J(y, \eta) = \int_{-a/2}^{a/2} dx \int_{-a/2}^{a/2} d\xi \cos\frac{\pi x}{a} \cos\frac{\pi\xi}{a} \left[\cos\beta \left(k^2 + \frac{\partial^2}{\partial x^2}\right) - \sin\beta \frac{\partial^2}{\partial x \partial y}\right] G(x, y | \xi\eta) \quad , \tag{89}$$

where $\frac{\partial^2}{\partial x^2}$ and $\frac{\partial}{\partial x}$ can be removed by partial integration. Then

$$J(y,\eta) = \cos\beta \left(k^2 - \frac{\pi^2}{a^2}\right) \iint_{a/2}^{a/2} dx d\xi \cos\frac{\pi x}{a} \cos\frac{\pi\xi}{a} \, G$$

$$+ \left(\frac{\pi}{a}\right) \cos\beta \int_{-a/2}^{a/2} d\xi \cos\frac{\pi\xi}{a} \left[G\left(x = \frac{a}{2}\right) + G\left(x = -\frac{a}{2}\right)\right]$$

$$- \left(\frac{\pi}{a}\right) \sin\beta \iint_{-a/2}^{a/2} dx d\xi \sin\frac{\pi x}{a} \cos\frac{\pi\xi}{a} \frac{\partial}{\partial y} \, G \quad , \tag{90}$$

where

$$G\left(x = \frac{a}{2}\right) = G(x, y: \xi, \eta)\Big|_{x = a/2} \quad .$$

To proceed further, some approximations of G are in order:

$$G(x,y;\xi,\eta)=\frac{e^{-jk\sqrt{(x-\xi)^2+(y-\eta)^2}}}{\sqrt{(x-\xi)^2+(y-\eta)^2}}\doteq\frac{e^{-jkr_o}}{r_o}\left\{1-\frac{x}{r_o}\cos(\alpha-\beta)-\frac{y}{r_o}\sin(\alpha-\beta)\right.$$

$$\left.+\frac{\xi}{r_o}\cos\alpha+\frac{\eta}{r_o}\sin\alpha\right\}\exp\left[-jkx\cos(\alpha-\beta)-jky\sin(\alpha-\beta)+jk\xi\cos\alpha+jk\eta\sin\alpha\right], \tag{91}$$

where r_o is the center-to-center distance of the two horn apertures.

The above is obtained as follows. By (69),

$$(x-\xi)^2+(y-\eta)^2=(r_o\cos\alpha+x\cos\beta-y\sin\beta-\xi)^2+(r_o\sin\alpha+x\sin\beta+y\cos\beta-\eta)^2$$

$$\doteq\left[r_o+x\cos(\alpha-\beta)+y\sin(\alpha-\beta)-\xi\cos\alpha-\eta\sin\alpha\right]^2 , \tag{92}$$

and

$$\frac{1}{\sqrt{(x-\xi)^2+(y-\eta)^2}}\doteq\frac{1}{r_o}\left(1-\frac{x}{r_o}\cos(\alpha-\beta)-\frac{y}{r_o}\sin(\alpha-\beta)+\frac{\xi}{r_o}\cos\alpha+\frac{\eta}{r_o}\sin\alpha\right) . \tag{93}$$

The substitution of (91) into (89) and straightforward integration gives:

$$J(y,\eta)=4\left(\frac{ka}{\pi}\right)^2\frac{e^{-jkr_o}}{r_o}\exp\left[-jky\sin(\alpha-\beta)+jk\eta\sin\alpha\right]\left\{\frac{C(\alpha-\beta)}{\phi(\alpha-\beta)}\frac{C(\alpha)}{\phi(\alpha)}\sin(\alpha-\beta)\sin\alpha\right.$$

$$+\frac{C(\alpha-\beta)}{\phi(\alpha-\beta)}\frac{C(\alpha)}{\phi(\alpha)}\sin(\alpha-\beta)\sin\alpha\left[\frac{\eta}{r_o}\sin\alpha-\frac{y}{r_o}\sin(\alpha-\beta)\right]$$

$$+j\frac{a}{2r_o}\left[\sin\alpha\cos\alpha\sin(\alpha-\beta)\frac{C(\alpha-\beta)}{\phi(\alpha-\beta)}\left(\frac{S(\alpha)}{\phi(\alpha)}-\frac{4ka}{\pi^2}\cos\alpha\frac{C(\alpha)}{\phi^2(\alpha)}\right)\right.$$

$$+\sin\alpha\sin(\alpha-\beta)\cos(\alpha-\beta)\frac{S(\alpha-\beta)}{\phi(\alpha-\beta)}\frac{C(\alpha)}{\phi(\alpha)}+\frac{4}{ka}\cos(\alpha-\beta)\frac{C(\alpha-\beta)}{\phi^2(\alpha-\beta)}\frac{C(\alpha)}{\phi(\alpha)}$$

$$\left.\left.\left(\cos\alpha-\frac{k^2a^2}{\pi^2}\cos\beta\cos(\alpha-\beta)\right)\right]\right\} , \tag{94}$$

where

$$C(\alpha-\beta)=\cos\left[\frac{ka}{2}\cos(\alpha-\beta)\right]$$

$$S(\alpha-\beta)=\sin\left[\frac{ka}{2}\cos(\alpha-\beta)\right]$$

$$\phi(\alpha-\beta)=1-\frac{k^2a^2}{\pi^2}\cos^2(\alpha-\beta) \quad . \tag{95}$$

$C(\alpha)$, $S(\alpha)$ and $\phi(\alpha)$ follow the same rule. From the above formulas for $J(y,\eta)$, a few conclusions valid for this physical problem can be extracted.

1) For large r_o and reasonably large α, the first term in the bracket is dominant.

2) For $\alpha=0$, there is only a near-field effect.

3) For small α, a combination of near- and far-fields exist.

In calculating the total power transmitted W_t, the presence of a receiving horn is again covered. Then, a real part of the complex Poynting vector integrated over the transmitting aperture will give the desired value, i.e.,

$$W_t=\frac{1}{2}\,\mathrm{Re}\int_A\int dS_A(\bar{E}\times\bar{H}_o^*)\cdot\hat{\xi}_o \tag{96}$$

where $\bar{H}_o$ is given by (71) and E is the assumed aperture field. Substituting all relevant values, there results:

$$W_t=-\frac{1}{2}\,\mathrm{Re}\int_A\int dS_A\iint dS'_A\left[\bar{E}(\bar{\rho}'_A)\times\hat{\xi}_o\right]^*\cdot\bar{\bar{Y}}_n^*(\bar{\rho}_A\rho'_A)\cdot\left[\bar{E}(\rho_A)\times\hat{\xi}_o\right]$$

$$=\mathrm{Re}\left[-\frac{\omega\mu\gamma}{2\pi^2 j\rho_o}\int_A\int dS_A\int_A\int dS'_A X^*(\eta')X(\eta)\right.$$

$$\left.\cos\frac{\pi\xi}{a}\cos\frac{\pi\xi'}{a}\left(k^2+\frac{\partial^2}{\partial x^2}\right)G(\xi,\eta,\xi',\eta')\right] . \tag{97}$$

Partial integration and change of integration variables leads to

$$W_t = \mathrm{Re}\left\{ -\frac{\omega\mu\gamma}{2\pi^2\rho_o j}\left(\frac{\pi}{a}\right)\left(\frac{ka}{\pi}\right)^2 \int_{-b/2}^{b/2} d\eta \int_{-b/2}^{b/2} d\eta' X^*(\eta') X(\eta) \right.$$

$$\left. \int_0^{\pi} d\lambda \left[\left(1+\frac{\pi^2}{k^2a^2}\right)\sin\lambda + \left(1-\frac{\pi^2}{k^2a^2}\right)\cos\lambda \right] \frac{\exp\left[+\frac{jka}{\pi}\sqrt{\frac{\pi^2}{a^2}(x-\xi)^2+\lambda^2}\right]}{\sqrt{\frac{\pi^2}{a^2}(x-\xi)^2+\lambda^2}} \right\}$$

$$= \mathrm{Re}\left[-\frac{\omega\mu\gamma}{j2\pi^2\rho_o}\left(\frac{\pi}{a}\right)\left(\frac{ka}{\pi}\right)^2 P \right] , \tag{98}$$

where

$$P = \int_{-b/2}^{b/2} d\eta \int_{-b/2}^{b/2} d\eta' X^*(\eta') X(\eta) \int_0^{\pi} d\lambda \left[\left(1+\frac{\pi^2}{k^2a^2}\right)\sin\lambda \right.$$

$$\left. + \left(1-\frac{\pi^2}{k^2a^2}\right)\cos\lambda \right] \frac{\exp\left[\frac{-jkb}{\pi}\sqrt{\frac{\pi^2}{a^2}(x-\xi)^2+\lambda^2}\right]}{\sqrt{\frac{\pi^2}{a^2}(x-\xi)^2+\lambda^2}} . \tag{99}$$

Since W_r is given by

$$W_r = \frac{1}{2}\frac{\omega\mu}{\gamma}|I|^2 , \tag{100}$$

the coupling formulas can be written as

$$C = \frac{W_r}{W_t} = 4\pi^2\left(\frac{\rho_o a}{r_o^2}\right)\frac{1}{\gamma^4 a^2 b^2} F \tag{101}$$

where

$$F = \frac{\left| \int_{-b/2}^{b/2} dy \int_{-b/2}^{b/2} d\eta X(\eta) X^*(y) J'(y, \eta) \right|^2}{\mathrm{Re}\,(jP)} , \tag{102}$$

where $J'(y, \eta)$ is the term inside the square bracket of equation (94) and P is given by (99). The integration of (102) in closed form seems to be impossible . However, for two very important cases, the relative values of coupling can be obtained without further integration.

For E-plane coupling (Fig. 1), i.e. $\alpha = \pi/2$, and r_o large,

$$J'(y,\eta) = \frac{C(\alpha-\beta)}{\phi(\alpha-\beta)} \frac{C(\alpha)}{\phi(\alpha)} \cos\beta = \frac{\cos(\frac{ka}{2}\sin\beta)}{(1-\frac{k^2a^2}{\pi^2}\sin^2\beta)} \cos\beta \quad . \tag{103}$$

Therefore,

$$C = C(\beta) = C_o \left| \int_{-b/2}^{b/2} X^*(y) e^{-jky\cos\beta} dy \right|^2 \left[\frac{\cos(\frac{ka}{2}\sin\beta)\cos\beta}{1-\frac{k^2a^2}{\pi^2}\sin^2\beta} \right]^2 \tag{104}$$

where

$$C_o = \frac{\left| \int_{-b/2}^{b/2} X(\eta) e^{ik\eta} d\eta \right|^2}{\mathrm{Re}(jP)} 4\pi^2 \left(\frac{\rho_o a}{r_o^2}\right) \frac{1}{\gamma^4 a^2 b^2} \tag{105}$$

C_o is independent of rotation angle β .

In this case, as indicated previously, the coupling has $1/r_o^2$ tendency . Thus, far-field coupling is dominant.

The β-dependence of (104) is compared with experimental results in Fig. 14.

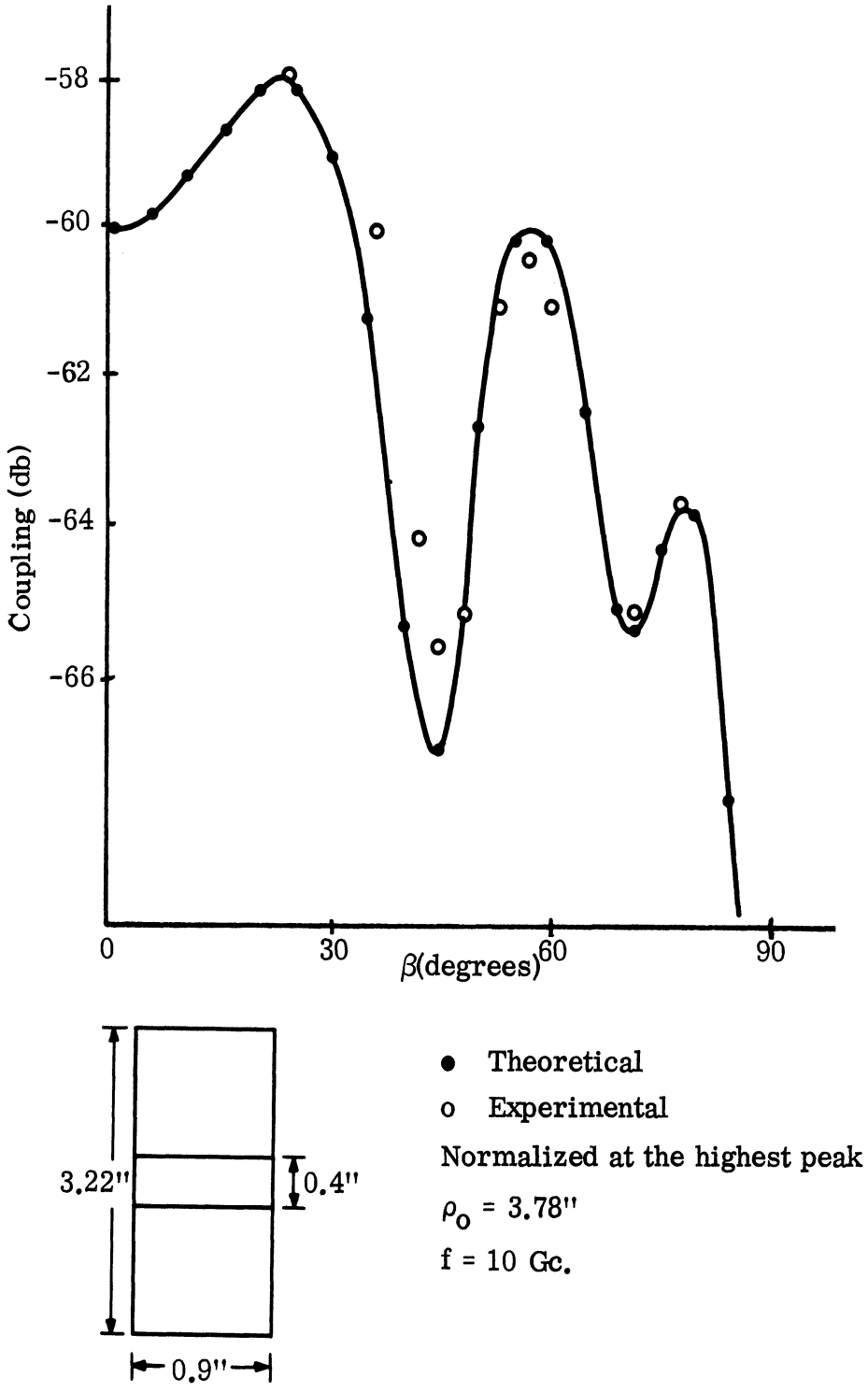

FIG. 14: ANGULAR DEPENDENCE OF COUPLING OF TWO HORNS

For H-plane coupling (α=0),

$$J'(y,\eta)=j\frac{a}{2r_o}\frac{4}{ka}\cos\beta\frac{C(\alpha-\beta)}{\phi^2(\alpha-\beta)}\frac{C(\alpha)}{\phi(\alpha)}\left(1-\frac{k^2a^2}{\pi^2}\cos^2\beta\right)$$

$$=j\frac{2}{kr_o}\frac{\cos\left(\frac{ka}{2}\cos\beta\right)}{\left(1-\frac{k^2a^2}{\pi^2}\cos^2\beta\right)}\frac{1}{\left(1-\frac{k^2a^2}{\pi^2}\right)}\cos\beta \qquad (106)$$

$$C=C(\beta)=C_1\left|\int_{-b/2}^{b/2}X^*(y)e^{jky\sin\beta}\right|^2\left[\frac{\cos\left(\frac{ka}{2}\cos\beta\right)\cos\beta}{1-\frac{k^2a^2}{\pi^2}\cos^2\beta}\right]^2 \qquad (107)$$

where

$$C_1=16\pi^2\left(\frac{\rho_o a}{k^2r_o^4}\right)\frac{1}{\gamma^4a^2b^2}\frac{1}{\left(1-\frac{k^2a^2}{\pi^2}\right)^2}\frac{\left|\int_{-b/2}^{b/2}X(\eta)d\eta\right|^2}{\mathrm{Re}(jP)}. \qquad (108)$$

In this case the coupling has $1/r_o^4$ tendency. It should be noted at this point that the above relation (107) is an incomplete one. The present situation is exactly the case where the second term inside the bracket of the numerator of equation (82) plays an important role which will be dealt with in the next report. However, the $1/r_o^4$ tendency does not change even when this new factor is considered.

III

EXPERIMENTAL COUPLING DATA

3.1 E- and H-Sectoral Horns

Experimental E- and H-plane coupling patterns for E- and H-sectoral horns are shown in Figs. 15 and 16 respectively. Patterns were measured at 8, 10 and 12 Gc. According to the theory for sectoral horn antennas, the coupling patterns should be symmetric with respect to the $\phi = 0^o$, $\pm 90^o$ and $\pm 180^o$ lines. The deviations shown in Figs. 15 and 16 are due to mechanical defects in the horns.

The E-sectoral horns used to obtain the patterns in Fig. 15 have an aperture size of 0.9x3.23" and a flare angle of 23^o (see θ_o in Fig. 2). The center-to-center spacing between the horns is 14.5". These horns were designed to have maximum gain at 8.8Gc near the center of the X-band source.

The H-sectoral horns used to obtain the patterns in Fig. 16 have an aperture size of 0.4x3.25" and a flare angle of 33^o (see θ_o in Fig. 5). The center-to-center spacing is 14.5". As in the case of the E-sectoral horns, these horns were designed to have maximum gain at a frequency of 8.8Gc.

It should be noted that the average levels of coupling decrease as the frequency increases. This is a result of the fact that the spacing between horns becomes larger in terms of wavelength as the frequency increases. It is interesting to note that the locations of local maxima and minima in these patterns do not change appreciably with changes in frequency. This effect is desirable when one is concerned with decoupling two such antennas .

If the H-plane curves in Figs. 15a and 15b for 8 and 10 Gc are compared, one sees that the lobe at $\phi = 90^o$ in Fig. 15a has been transformed into three lobes in Fig. 15b. In Fig. 15c these new lobes become more pronounced. This increases in the

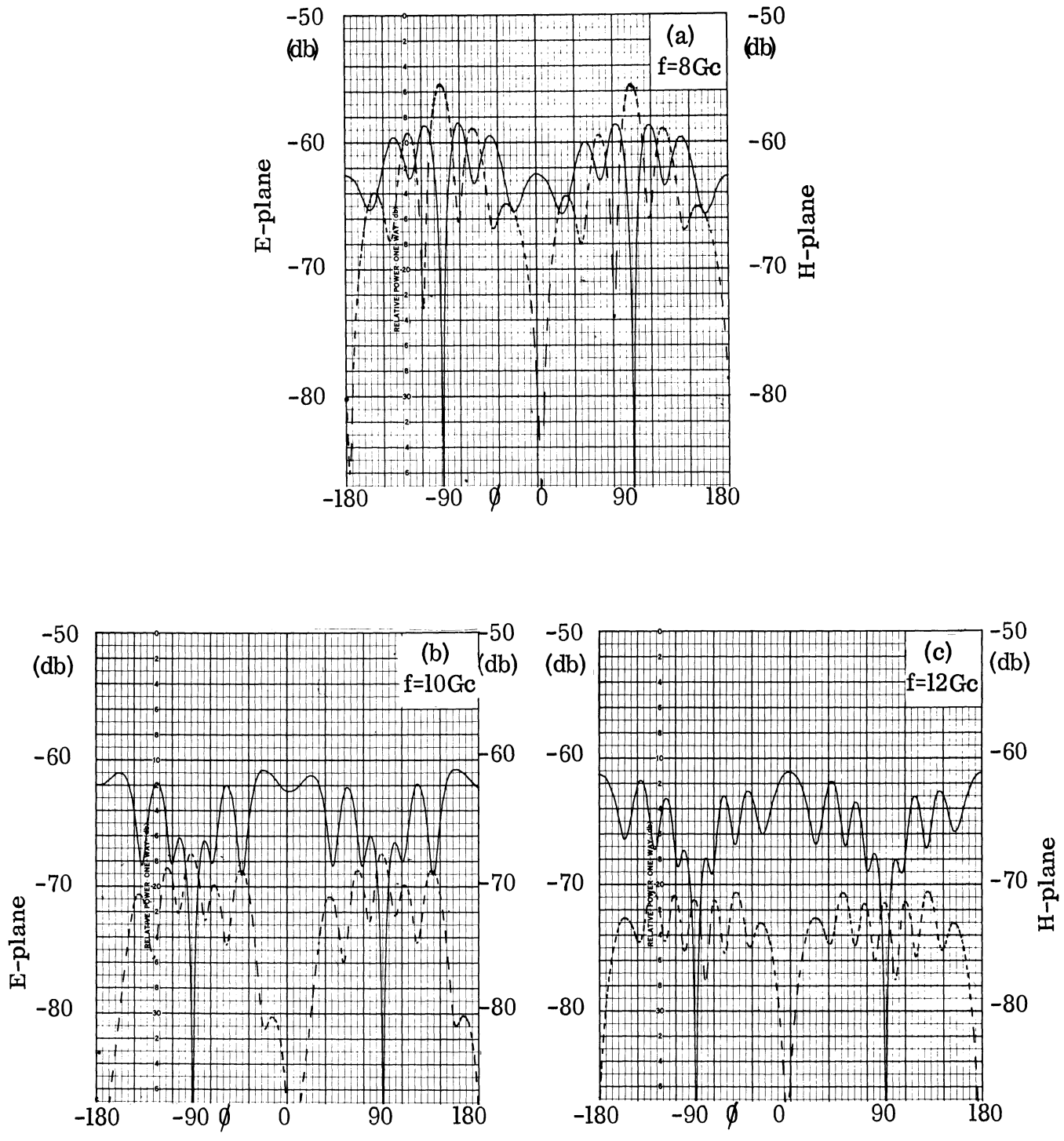

FIG. 15: E-SECTORAL HORN COUPLING PATTERNS
(——)E-PLANE. (---) H-PLANE.

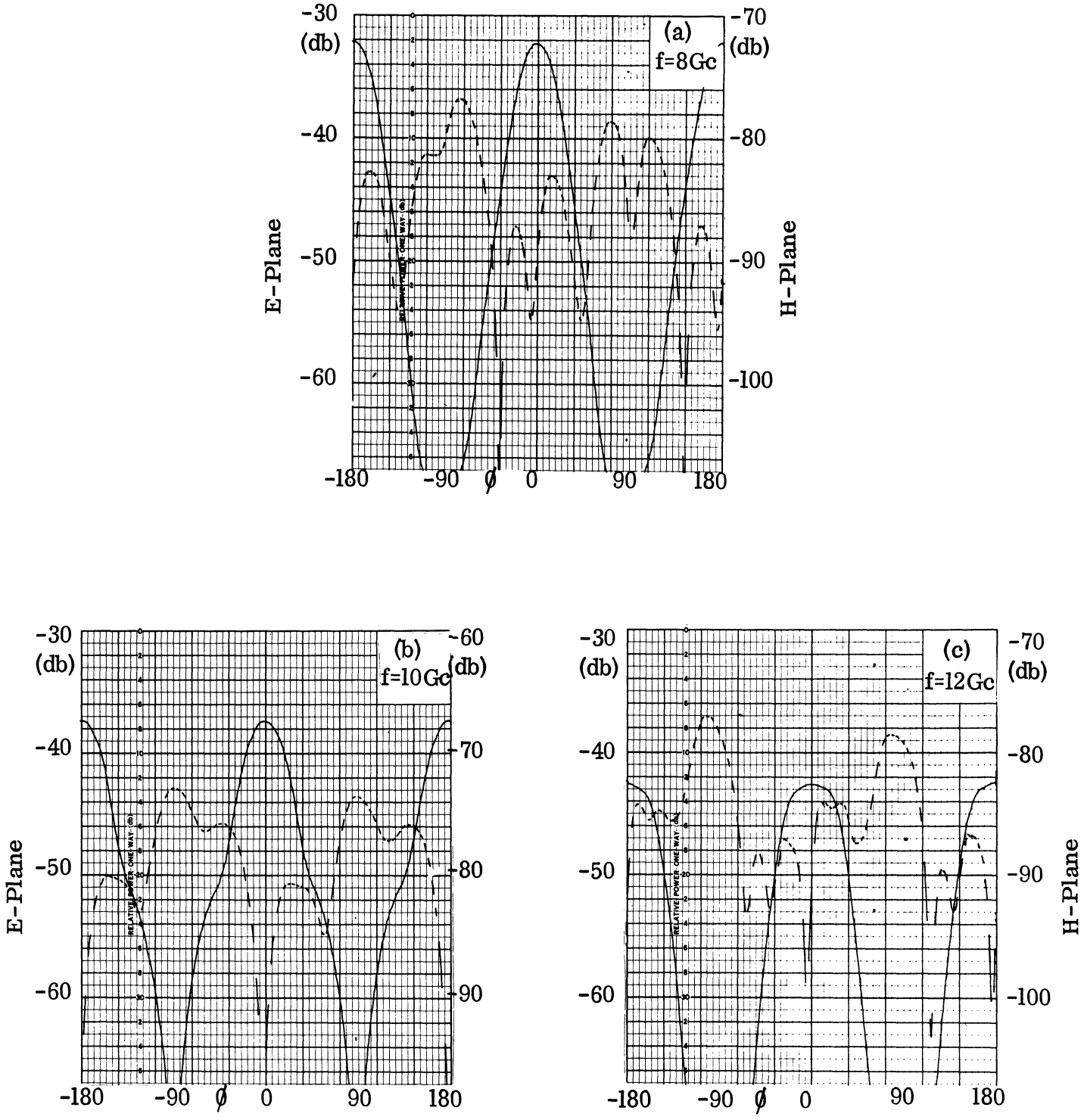

FIG. 16: H-SECTORAL HORN COUPLING PATTERNS. (—)E-PLANE, (---)H-PLANE.

variation of the coupling patterns as the frequency is increased is due to the increase in the size of the horn aperture in terms of wavelengths and the resulting increase in phase cancellation which occurs in the radiated field. The lobe splitting effect is also evident in the E-plane curves of Figs. 15a and 15b. Here the lobe at $\phi=0^{o}$ in Fig. 15a splits into lobes in Fig. 15b leaving a local minimum in the coupling pattern at $\phi=0^{o}$.

3.2 Conical and Pyramidal Horns

Experimental data were gathered for a pair of conical horns mounted in a ground plane with L=26.4 cm, a=4.6, $\theta_{o}=9.9^{o}$ (see Fig. 9). The gain of these horns is 18 db at 9 Gc. The data were taken for the linearly polarized case at 8, 10 and 12 Gc, at a center-to-center spacing of 36.6 cm. The two curves shown in each of Figs. 17a to 17c, labelled E-plane and H-plane coupling, are described by the geometry of Fig. 1. It is seen from these curves that, indeed, as predicted by the analysis the coupling levels vary as $\sin\phi$. The maxima of the H-plane coupling are down 6 to 16 db from the maxima obtained for the E-plane coupling. At this spacing of 36.6 cm, the lowest coupling levels obtainable for the linearly polarized pairs of conical horns is about -90 db. Figure 18 shows the E-plane coupling pattern as a function of rotation angle ϕ (of the receiving horn) at 8 Gc with both horns circularly polarized. Because of the phase quadrature relationship between the two orthogonal components existing in the horns, the nulls of the coupling patterns disappear. The slight variations in coupling are due to the aperture fields being somewhat elliptically polarized.

A pair of pyramidal horns mounted in a ground plane was also tested at the same center-to-center spacing of 36.6 cm. These horns were fed from X-band waveguide (1.01x2.28cm), which was flared out over a length of 10.1cm to an opening of 4.77x6.04cm. The horns have a gain of about 12 db at 9 Gc. Figures 19a through 19c show both the E- and H-plane coupling curves. The coupling pattern for the E-plane

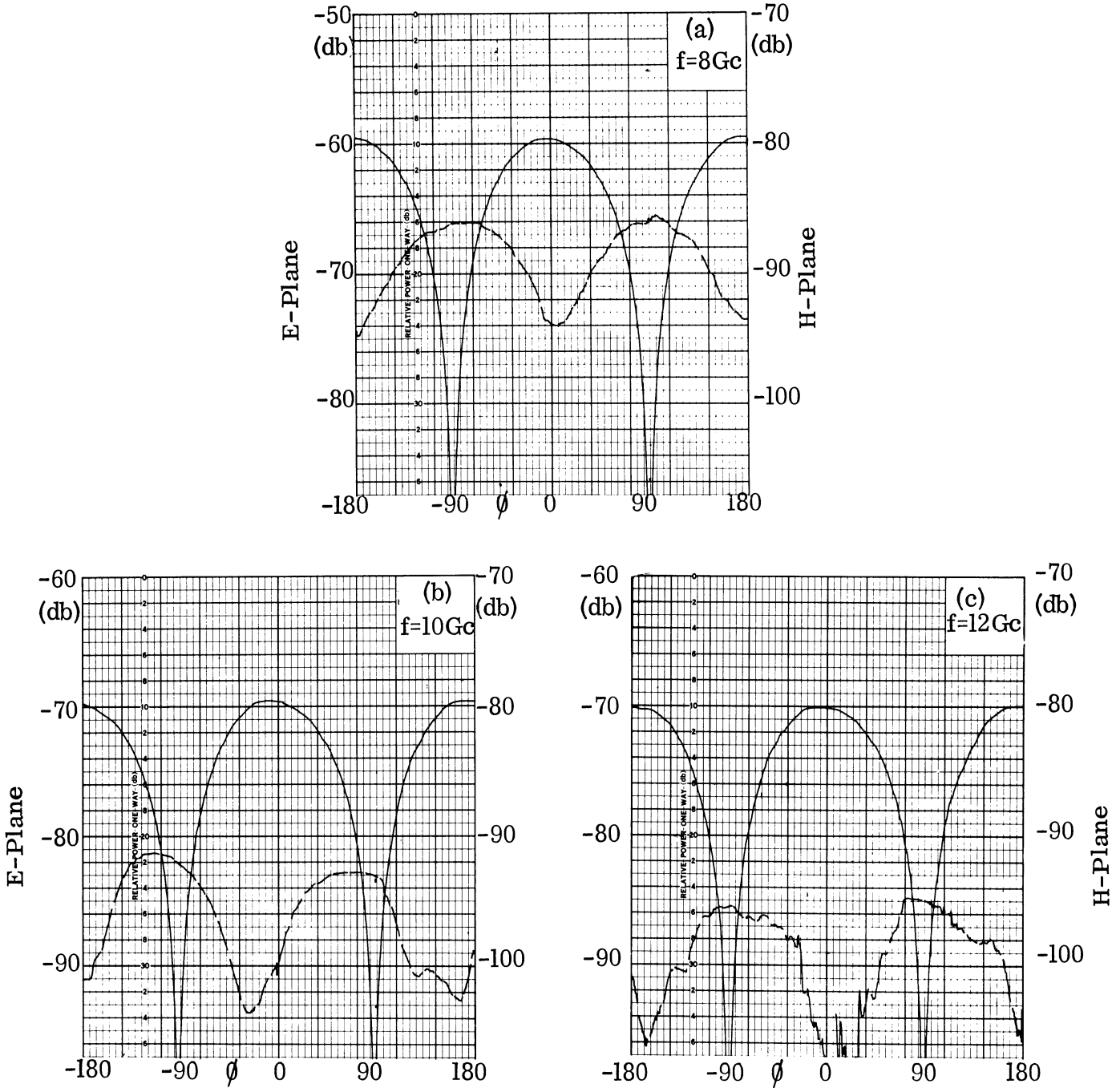

FIG. 17: CONICAL HORN COUPLING PATTERNS (LINEARLY POLARIZED)
(—) E-PLANE, (---)H-PLANE.

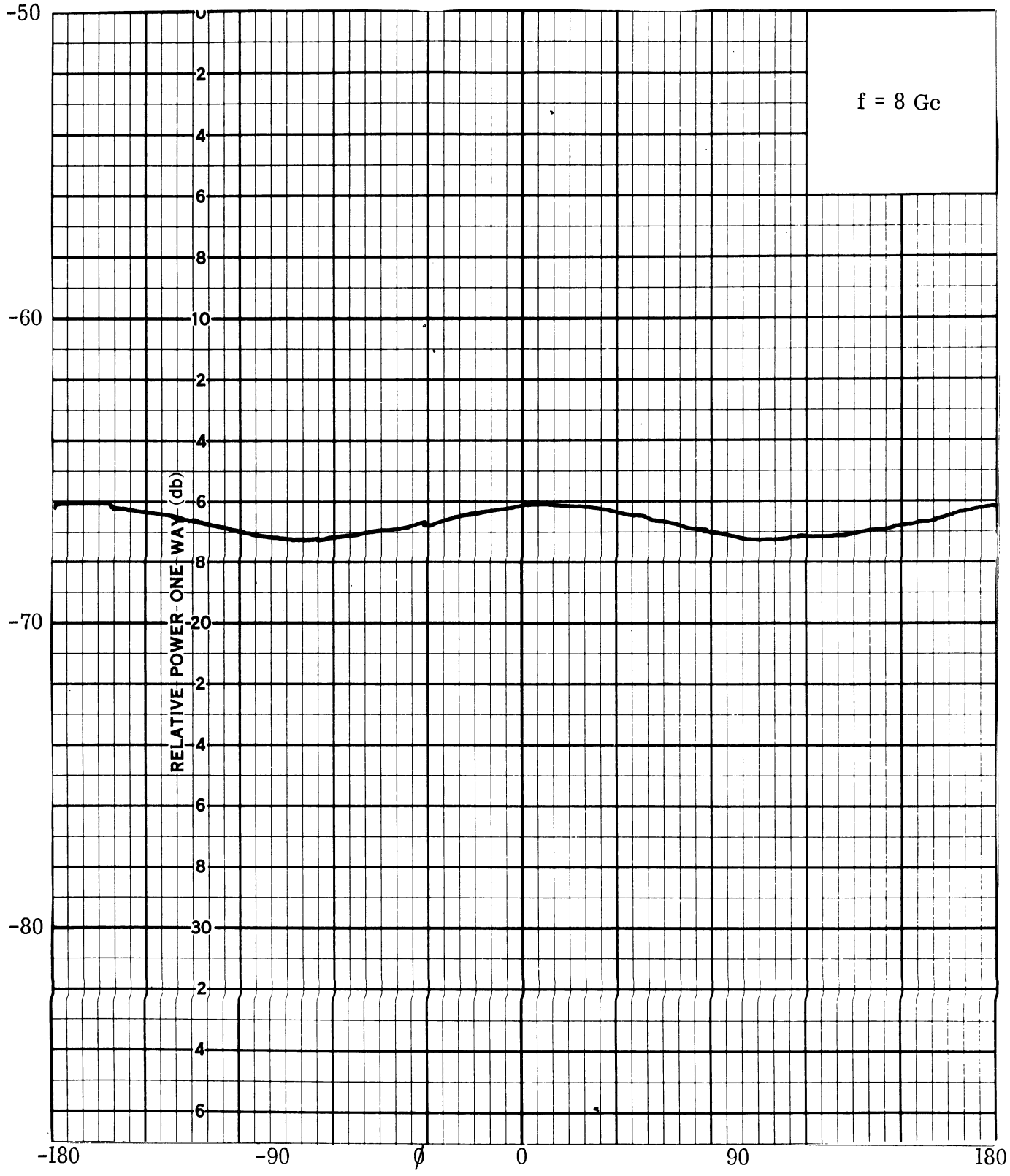

FIG. 18: CIRCULARLY POLARIZED CONICAL HORN COUPLING PATTERN

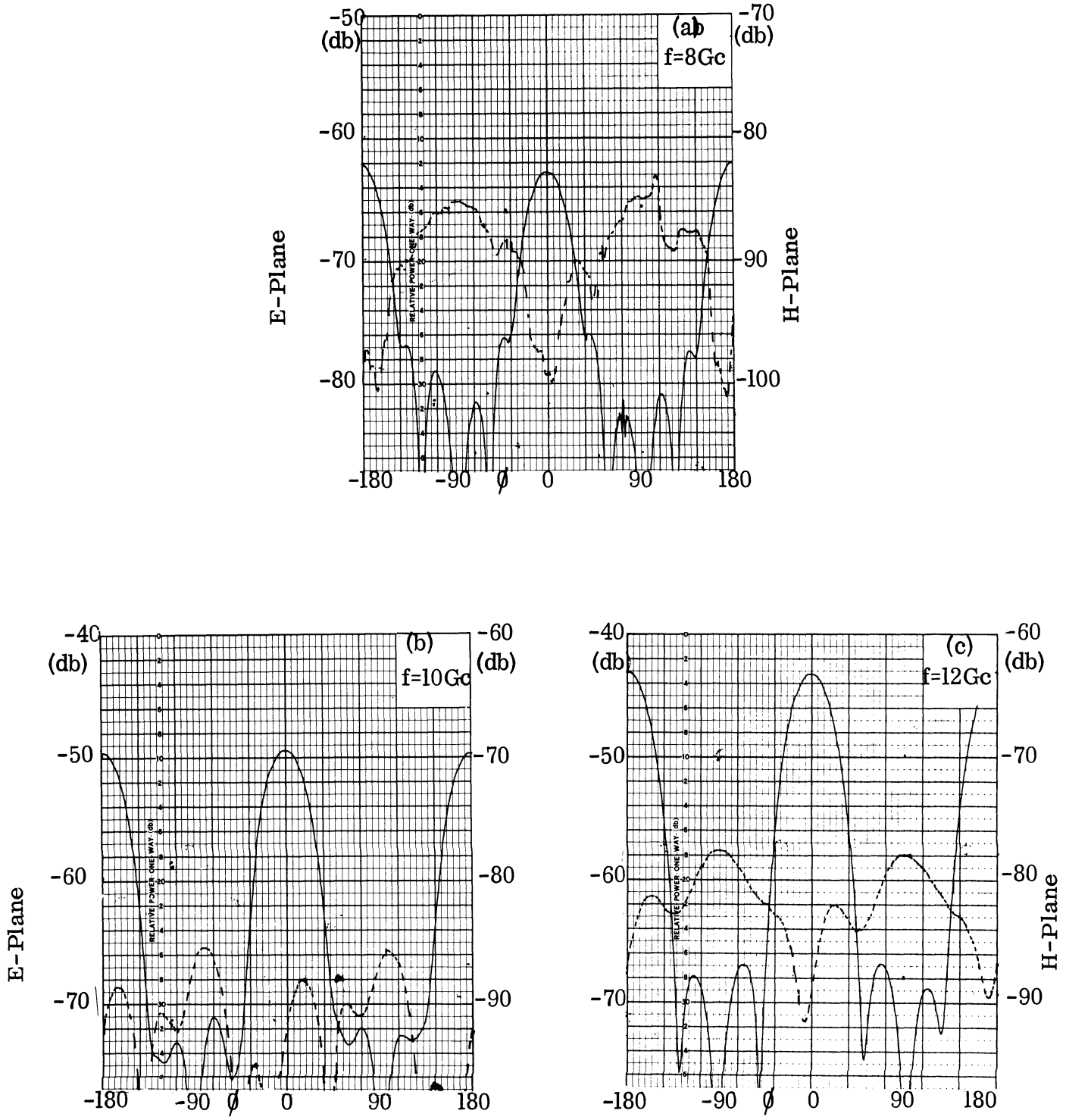

FIG. 19: PYRAMIDAL HORN COUPLING PATTERNS. (—)E-PLANE, (---) H-PLANE.

case is more directional than for the conical horns because there is more tapering of the E-field in the pyramidal horn aperture. It is to be noted that this more selective coupling occurs even though the conical horns have a much larger aperture, and correspondingly, much higher gain. Due to the lower level of the 'sidelobes' in the ground plane for the pyramidal horns, an antenna designer might want to consider using a pyramidal horn instead of a conical horn to achieve lower coupling levels between adjacent horns.

IV

CONCLUSIONS

So far the coupling data on a variety of antennas have clearly demonstrated the existence of a wide range of coupling values. The coupling level of spiral antennas is on the order of -30 db while the coupling levels of some of the horn type antennas having the H lines co-linear is less than -75 db. Thus some of the antennas now under study will show levels below the -75 db level of interest stipulated in the contract, at least for some spacings of the antennas. The -75 db level is believed to be a realistic limit for coupling measurements in a free space environment. Evidence now indicates that in a real life situation, effects due to scattering will be predominant for antennas having an intrinsic coupling level of -75 db. It should be noted that the coupling values which have been observed for a variety of antennas studied to date are far below levels commonly reported in the literature.

Theoretical expressions have been developed for the coupling between E and H-sectoral horns using an approach applicable for far field only and by a second approach valid for both near and far regions. Good experimental verification has been achieved for these results. Theoretical expressions have also been derived for far field coupling between conical horns.

V

FUTURE WORK

To date the required experimental and theoretical effort has largely been accomplished for rectangular slot antennas, spiral antennas, and horn type antennas. In the remaining time it is expected that experimental work will be performed on a trough waveguide-type of traveling wave antenna and on recessed conical spiral antennas. The latter, it is anticipated, will be handled very much like the earlier spiral antenna work. Finally, during this period it is expected that coupling of scimitar antennas will be studied. This latter study will be very interesting because of the broad pattern of the scimitar and the multipolarization situation which exists.

It is planned to give more attention to the influence of independent scatterers on the coupling between antennas. It is believed that two horn antennas appropriately spaced and mounted on a common ground plane on an aerospace vehicle may not have sufficient direct coupling for significant interference, but that problems will occur due to scattering from one type of protuberance or another. The interference effects due to scattering from objects in the anechoic room during coupling measurements have helped to show the importance of considering their effects.

The detailed organization of the data acquired so far is a major objective in future work. Our present plans call for the presentation of data on rectangular slot antennas as well as circular and square Archimedean spiral antennas in a variety of nomograph charts. A separate nomograph will be made for each type of antenna. A typical nomograph for the circular Archimedean spiral antenna will predict the coupling for a given spacing and orientation angle of the second antenna with respect to the first. The bar scales in the nomograph will be on a normalized basis wherever possible. In order that the nomograph can be used for all designs of circular Archimedean spirals, it is possible that a supplementary nomograph involving the design details including spacing of the elements of the spiral may be utilized.

Nomographs for the square Archimedean spiral would, no doubt, be very similar to those for the circular Archimedean spiral. A nomograph for the coupling of rectangular slot antennas would probably be somewhat simpler to design than those for the Archimedean spirals. It now appears that one simple nomograph taking into account the actual dimensions of the slot as well as the frequency of operation would be sufficient.

In the cases of the antennas described above, it is contemplated that it will not be necessary to do much smoothing or averaging of the experimental curves. However, it appears that it will be necessary to average the experimental curves obtained for circular or rectangular horns in order to avoid the use of a double-valued scale on the nomograph. Simplicity in the construction of a nomograph precludes multiple valued functions. In addition to the antennas already cited, it is contemplated that coupling data for monopole antennas erected perpendicularly to a common ground plane will be presented in nomograph form. This appears to be straightforward at the present time.

One of the more useful methods for the presentation of the data may very well be by means of a computer program. The possibility of preparing a program for the coupling between various rectangular and conical horns will be investigated. It is believed that one program will be sufficient for any and all rectangular horns. This program will be written in a standard programming language. During the next few weeks, a decision will be made in cooperation with the sponsor regarding the choice of the programming language.

REFERENCES

Khan, P. J., et al (1964), "Derivation of Aerospace Antenna Coupling-Factor Interference Prediction Techniques," The University of Michigan Cooley Electronics Laboratory Report No. 4957-8-F.

Lewin, L. (1951), Advanced Theory of Waveguides, Iliffe Publishing Company Company, London, p. 123.

Potter, P. D. (1963), "A New Horn Antenna with Suppressed Sidelobes and Equal Beamwidths," Microwave Journal, pp. 71-78, June 1963.

Silver, S. (1949), Microwave Antenna Theory and Design, McGraw-Hill, New York, pp. 336-337.

Stratton, J. A. (1941) Electromagnetic Theory, McGraw-Hill, New York, pp. 29 and 431.